Bone marrow transplantation generates T cell–dependent control of myeloma in mice

Slavica Vuckovic,[1,2,3] Simone A. Minnie,[1,2] David Smith,[1] Kate H. Gartlan,[1,2,4] Thomas S. Watkins,[1] Kate A. Markey,[1,2,5] Pamela Mukhopadhyay,[1] Camille Guillerey,[1,2] Rachel D. Kuns,[1] Kelly R. Locke,[1] Antonia L. Pritchard,[1,6] Peter A. Johansson,[1] Antiopi Varelias,[1,2] Ping Zhang,[1] Nicholas D. Huntington,[7,8,9] Nicola Waddell,[1] Marta Chesi,[10] John J. Miles,[11] Mark J. Smyth,[1] and Geoffrey R. Hill[1,4,12,13]

[1]QIMR Berghofer Medical Research Institute, Brisbane, Australia. [2]Faculty of Medicine, The University of Queensland, Herston, Australia. [3]Multiple Myeloma Research Group, Institute of Haematology, Royal Prince Alfred Hospital, Camperdown, Australia. [4]Clinical Research Division, Fred Hutchinson Cancer Research Center, Seattle, Washington, USA. [5]Division of Immunology, Memorial Sloan Kettering Cancer Center, New York, New York, USA. [6]Genetics and Immunology, University of the Highlands and Islands, Inverness, United Kingdom. [7]Molecular Immunology Division, Walter and Eliza Hall Institute of Medical Research, Parkville, Australia. [8]Department of Medical Biology and [9]Faculty of Medicine, Dentistry and Health Sciences, The University of Melbourne, Melbourne, Australia. [10]Comprehensive Cancer Center, Mayo Clinic, Scottsdale, Arizona, USA. [11]Centre for Biodiscovery and Molecular Development of Therapeutics, Australian Institute of Tropical Health and Medicine (AITHM), James Cook University, Cairns, Australia. [12]Department of Haematology, The Royal Brisbane and Women's Hospital, Brisbane, Australia. [13]Division of Medical Oncology, University of Washington, Seattle, Washington, USA.

Transplantation with autologous hematopoietic progenitors remains an important consolidation treatment for patients with multiple myeloma (MM) and is thought to prolong the disease plateau phase by providing intensive cytoreduction. However, transplantation induces inflammation in the context of profound lymphodepletion that may cause hitherto unexpected immunological effects. We developed preclinical models of bone marrow transplantation (BMT) for MM using Vk*MYC myeloma–bearing recipient mice and donor mice that were myeloma naive or myeloma experienced to simulate autologous transplantation. Surprisingly, we demonstrated broad induction of T cell–dependent myeloma control, most efficiently from memory T cells within myeloma-experienced grafts, but also through priming of naive T cells after BMT. $CD8^+$ T cells from mice with controlled myeloma had a distinct T cell receptor (TCR) repertoire and higher clonotype overlap relative to myeloma-free BMT recipients. Furthermore, T cell–dependent myeloma control could be adoptively transferred to secondary recipients and was myeloma cell clone specific. Interestingly, donor-derived IL-17A acted directly on myeloma cells expressing the IL-17 receptor to induce a transcriptional landscape that promoted tumor growth and immune escape. Conversely, donor IFN-γ secretion and signaling were critical to protective immunity and were profoundly augmented by CD137 agonists. These data provide new insights into the mechanisms of action of transplantation in myeloma and provide rational approaches to improving clinical outcomes.

Introduction

Multiple myeloma (MM) is a bone marrow–based (BM-based) plasma cell neoplasm that often evolves from a premalignant stage, known as monoclonal gammopathy of undetermined significance (MGUS), to present with characteristic features including cytopenias, hypercalcemia, lytic bone lesions, and renal impairment (1). The malignant plasma cell is clonal and usually generates a monoclonal paraprotein that can be quantified in sera and serves as a sensitive disease marker. Treatment characteristically involves the administration of cycles of immunomodulators and/or a proteosome inhibitor with steroids and an alkylating agent until a maximal disease response is achieved. At this point, stem cell mobilization, collection, and cryopreservation are undertaken, and cells are reinfused after high-dose chemotherapy in a therapeutic consolidation step that is known to prolong the disease plateau phase, induce higher complete response rates, and improve progression-free survival (2, 3). Indeed, stem cell transplantation (SCT) remains a standard of care for MM patients of appropriate age and performance status (4, 5). The growing number of patients undergoing SCT in states of minimal residual disease (MRD) has resulted in an increasing proportion that enjoy long-term complete remission (CR). Intriguingly, survival plateaus that were previously only demonstrable in patients with immune-mediated graft-versus-myeloma effects after allogeneic SCT are now seen in certain subgroups of patients after autologous SCT (6). Nevertheless, even in an era of an abundance of new therapeutic agents and SCT, resistance to treatment usually ensues, and the majority of patients with MM relapse and die of progressive disease.

It is generally presumed that the therapeutic benefit of myeloablative chemotherapy and autologous SCT is a result of intensive cytoreduction (7). Nevertheless, this therapy invokes significant

▶ Related Commentary: p. 48

Authorship note: SV and SAM contributed equally to this work.
Conflict of interest: GRH has received funding from Roche for clinical trials of IL-6 inhibition in transplantation. MJS has research agreements with Bristol-Myers Squibb, Tizona Therapeutics, and Aduro Biotech.

Submitted: November 28, 2017; **Accepted:** October 2, 2018.
Reference information: *J Clin Invest*. 2019;129(1):106–121.
https://doi.org/10.1172/JCI98888.

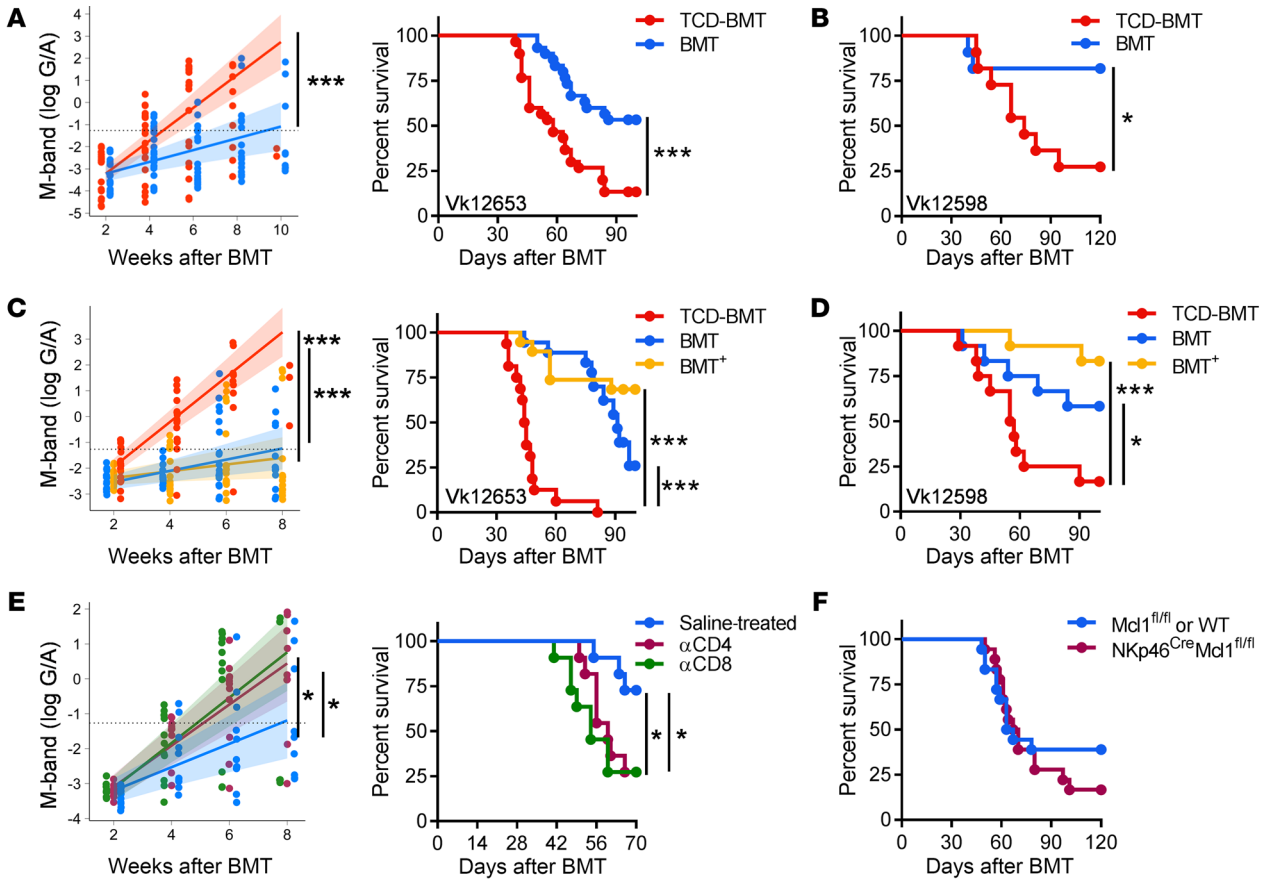

Figure 1. Donor T cells provide immune-mediated control of myeloma after BMT. MM-bearing recipients were lethally irradiated and transplanted with 10 × 10^6 BM cells with or without 5 × 10^6 T cells from naive or myeloma-experienced donors. Mice were monitored for survival and tumor burden using M-band (G/A) levels. M-band levels were modeled to calculate a predictive rate of tumor growth (solid line), with shaded CIs and the M-band relapse threshold shown as a dotted line. (**A**) Tumor burden and survival of Vk12653-bearing recipients (n = 30; combined from 5 experiments) and (**B**) survival of Vk12598-bearing recipients (n = 10; combined from 2 experiments) that received TCD-BMT or BM and T cells from naive donors (BMT). (**C**) Tumor burden and survival of Vk12653-bearing recipients (n = 16–19 combined from 3 experiments) and (**D**) survival of Vk12598-bearing recipients (n = 12 combined from 2 experiments) transplanted with TCD-BMT, BMT, or TCD-BM with myeloma-experienced T cells (BMT$^+$). (**E**) Tumor burden and survival of Vk12653-bearing recipients treated with saline or CD8- or CD4-depleting Abs (αCD8, αCD4) from day 0 to 8 weeks after BMT (n = 11 combined from 2 experiments). (**F**) Survival of Vk12653-bearing recipients of BMT grafts from NK cell–intact (Mcl1$^{fl/fl}$ or WT) or NK cell–deficient (NKp46^{Cre}Mcl1$^{fl/fl}$) donors (n = 18 combined from 2 experiments). To determine statistical significance, the tumor burden was plotted using longitudinal mixed-effects linear models, and survival was analyzed using a log-rank test. *P < 0.05 and ***P < 0.001.

inflammation and profound lymphodepletion that may result in unappreciated immunological effects after SCT. To investigate this further, we explored the mechanisms of efficacy of SCT in a preclinical model of myeloma using recipient mice bearing Vk*MYC myeloma and radiation-based conditioning with BM as a source of stem cells. Although most clinical autologous SCT for myeloma now utilizes high-dose melphalan rather than total body irradiation (TBI), this results in similar states of inflammation and lymphodepletion (8). Our data provide evidence of the induction of profound T cell–mediated myeloma control after transplantation and offer therapeutic approaches targeting IL-17A and CD137 costimulation to enhance myeloma-immune equilibrium and improve cure rates.

Results

Donor T cells provide immune-mediated control of myeloma after BM transplantation. To determine the factors influencing myeloma control after BM transplantation (BMT), we developed preclinical models (9) in which Vk*MYC myeloma–bearing B6 recipient mice (Vk12653 clone, unless otherwise stated) were lethally irradiated and transplanted with T cell–depleted BM (TCD-BM), without T cells (TCD-BMT), or with T cells from myeloma-naive (BMT) or myeloma-experienced (BMT$^+$) B6 donors, respectively (see Supplemental Figure 1A; supplemental material available online with this article; https://doi.org/10.1172/JCI98888DS1). Myeloma burdens after BMT were determined by quantifying monoclonal paraprotein (M-band) in the sera, expressed as a ratio of γ-globulin/albumin (G/A), as previously described (10). The kinetics of M-band progression was mathematically modeled over time to generate predictions of myeloma growth as detailed in the Methods. We defined a quantitative M-band threshold (G/A = 0.28), at which point all animals would reliably develop progressive myeloma. Polyclonal plasma cells and monoclonal myeloma cells in the BM and spleens of naive and MM-bearing mice, respectively, were classified as CD138$^+$CD19$^-$, however, myeloma cells expressed lower levels of MHC class II (MHC-II) and higher levels of MHC class I (MHC-I) and CD155, and all expressed PD-L1 (Supplemental Figure 1B).

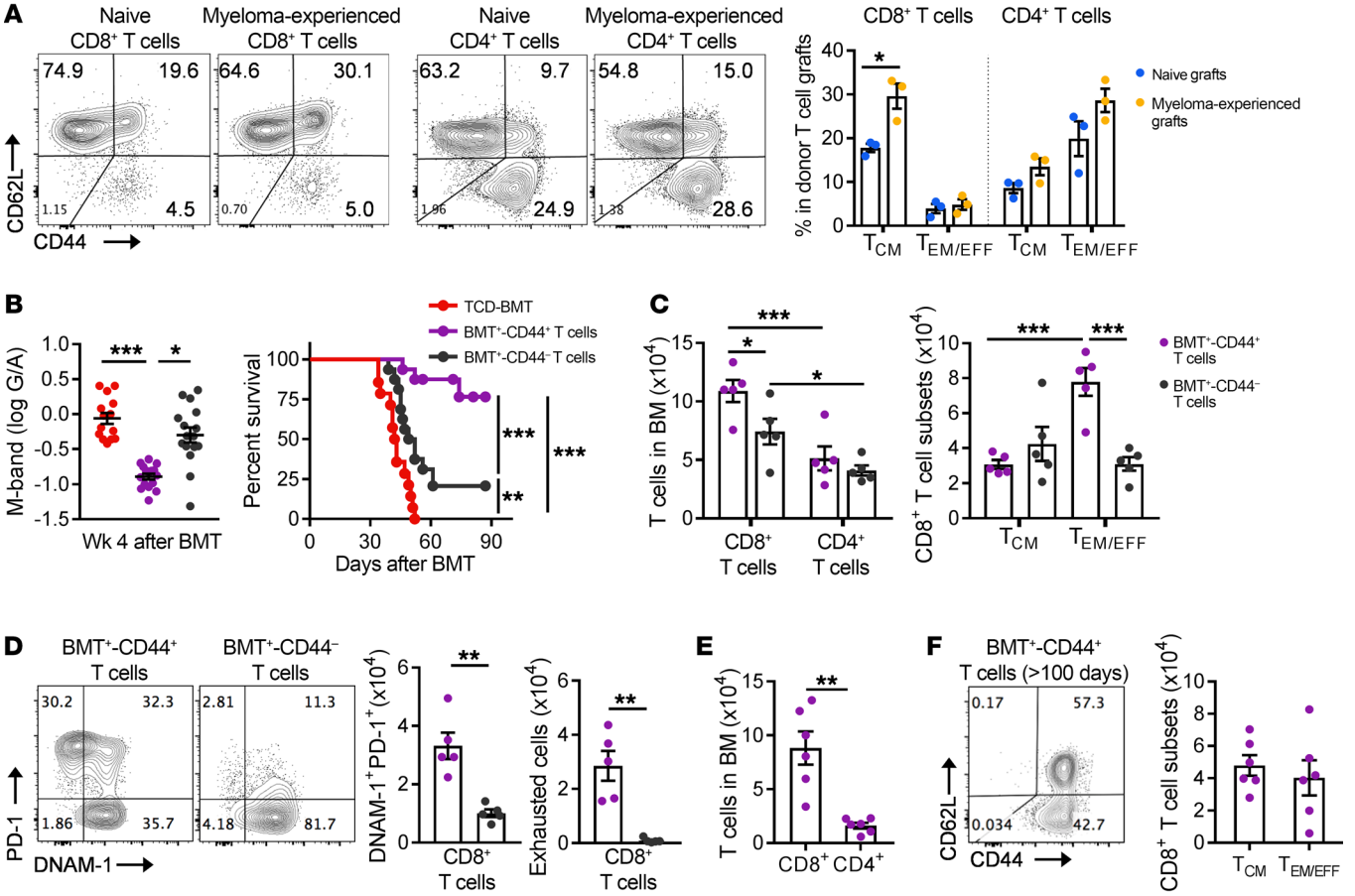

Figure 2. Donor memory T cells limit myeloma progression after BMT with myeloma-experienced T cells. (**A**) Representative FACS plots and frequency of T_{CM} ($CD44^+CD62L^+$) and $T_{EM/EFF}$ ($CD44^+CD62L^-$) cells in naive and myeloma-experienced donor grafts (*n* = 3 per group). (**B**–**F**) MM-bearing recipients were lethally irradiated and transplanted with 10 × 10^6 TCD-BM cells alone (TCD-BMT) or 3 × 10^6 $CD44^+$ or $CD44^-$ T cells from CD45.1/CD45.2 myeloma-experienced donors. (**B**) Tumor burden, quantified and modeled using M-band levels as described, and survival of Vk12653-bearing recipients (*n* = 14–16 combined from 2 experiments). (**C** and **D**) Recipients were sacrificed 2 weeks after BMT^+, and BM T cells were analyzed by flow cytometry (*n* = 5 per group from 1 experiment). (**C**) Absolute numbers of donor $CD8^+$ and $CD4^+$ T cells and T_{CM} and $T_{EM/EFF}$ $CD8^+$ T cells in BM. (**D**) Representative FACS plots and absolute numbers of DNAM-1^+PD-1^+ and exhausted (DNAM-1^-PD-1^+TIM-3^+) donor $CD8^+$ T cells. (**E** and **F**) Recipients of BMT^+-$CD44^+$ grafts were sacrificed more than 100 days after BMT^+, and BM T cells were analyzed via flow cytometry (*n* = 6 from 1 experiment). (**E**) Absolute numbers of donor $CD8^+$ and $CD4^+$ T cells. (**F**) Representative FACS plot and absolute numbers of T_{CM} and $T_{EM/EFF}$ donor $CD8^+$ T cells. Data represent the mean ± SEM. *$P < 0.05$, **$P < 0.01$, and ***$P < 0.001$, by log-rank test for survival data and Mann-Whitney *U* test for 2-sample and ANOVA for multiple-sample comparisons.

In this preclinical model, we found that MM-bearing recipients of BM and T cells from naive donors (BMT) had significantly improved control of both Vk12653 and Vk12598 myeloma cell clones compared with recipients of T cell–depleted grafts (TCD-BMT), with reduced M-band progression and improved survival (Figure 1, A and B). We next compared myeloma progression in MM-bearing recipients of TCD-BMT, TCD-BM with naive T cells (BMT), or T cells from myeloma-experienced donors (BMT^+). Myeloma-experienced donors had low myeloma burden (M-bands <0.28), analogous to the MRD state that is characteristically induced by chemotherapy in patients prior to clinical stem cell collection. We observed that control of both myeloma cell clones was significantly improved in both BMT and BMT^+ recipient mice compared with TCD-BMT recipient mice (Figure 1, C and D). Interestingly, we observed no significant difference in myeloma control between BMT and BMT^+ recipients. Depletion of either $CD4^+$ or $CD8^+$ T cells after BMT increased the rate of tumor growth and reduced survival compared with saline-treated recipient mice (Figure 1E), suggesting that both T cell subsets play an important role in disease control after BMT. Donor γδ and NK T cells were not required for antimyeloma immunity, as genetic deletion of these cells (i.e., $TCR\delta^{-/-}$ and $J\alpha18^{-/-}$, respectively) in donor grafts had no impact on myeloma progression (Supplemental Figure 2, A and B). To determine whether NK cells provided immunological control of myeloma after BMT, we next transplanted grafts from donor mice that lacked the capacity to generate mature NK cells ($NKp46^{cre}Mcl1^{fl/fl}$; Supplemental Figure 3A and ref. 11). Surprisingly, we found that NK cell deficiency had no impact on myeloma burden (Supplemental Figure 3B) or survival (Figure 1F). These results highlight the observation that control of myeloma after BMT is not simply a consequence of cytoreductive therapy and involves a significant T cell–dependent immunological component, consistent with the establishment of myeloma-immune equilibrium. Given the susceptibility of Vk*-MYC myeloma to immune control, we sought to understand the nonsynonymous variation among the transplanted MM cells and

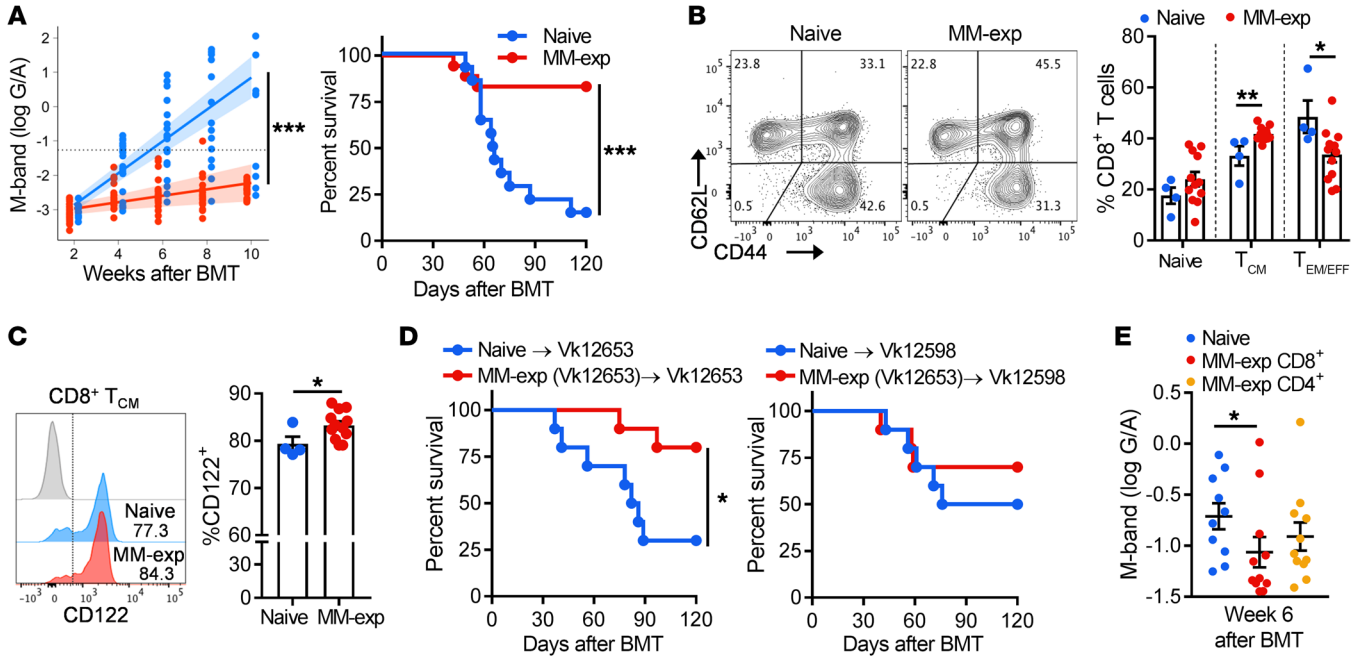

Figure 3. BMT generates protective myeloma-specific T cells. MM-bearing recipients were transplanted with TCD-BM from naive mice and either naive T cells (naive) or T cells from MM-bearing recipients with long-term control of Vk12653 myeloma (>120 days after BMT: MM-exp). (**A**) Tumor burden, quantified and modeled using M-band levels as described, and survival of Vk12653-bearing recipients transplanted with either naive or MM-exp T cells (n = 14–18 combined from 2 experiments). (**B**) Representative FACS plots and frequency of $T_{EM/EFF}$, T_{CM}, and naive CD8$^+$ T cells and (**C**) representative histograms and frequency of CD122$^+$ cells within T_{CM} CD8$^+$ T cells in the BM of recipients of naive or MM-exp T cells, 120 days after BMT (naive, n = 4; MM-exp, n = 12 from 1 experiment). (**D**) Survival of Vk12653-bearing recipient mice and Vk12598-bearing recipient mice transplanted with naive TCD-BM and either naive T cells or MM-expT cells from mice with long-term control of Vk12653 myeloma (n = 10 combined from 2 experiments). (**E**) M-band 6 weeks after BMT of secondary recipients of naive TCD-BM and either naive T cells or 2 × 10^6 MM-exp CD8$^+$ or 2 × 10^6 MM-exp CD4$^+$ T cells transferred with naive CD4$^+$ or CD8$^+$ T cells, respectively (n = 10–11 combined from 2 experiments). Data represent the mean ± SEM. *P < 0.05, **P < 0.01, and ***P < 0.001, by Mann-Whitney U test for numerical values and log-rank test for survival data.

the recipient mice, since, in patients, a higher mutation burden appears to cause susceptibility to immune control but is associated with a worse clinical outcome (12). We thus performed whole-exome sequencing using the translated region, which accounts for 34,300,425 bp in GRCm38(mm10), as the basis of the assessment of variation among tumor and recipient cells. After applying filtering criteria (as outlined in the Supplemental Methods), we noted that 950 coding region variants were present, including 375 nonsynonymous variants. These data allowed the direct comparison of the burden of nonsynonymous variants in Vk12653 myeloma (11.09 per Mb) with 3 published sequencing projects on human MM (0.03–20.7 per Mb) (12–14). Given that the Vk12653 burden was within the range, albeit in the upper quartile, of that reported for human MM, this is a relevant myeloma model.

T cell–dependent myeloma control after BMT with myeloma-experienced T cells is the consequence of preexisting myeloma immunity. Next, we investigated whether de novo priming of naive donor T cells after BMT or the presence of preexisting T cell antitumor memory in the donor graft contributed to myeloma control after BMT$^+$. In support of the latter, we observed a significant increase in the frequency of CD62L$^+$CD44$^+$ central memory T cells (T_{CM}) in myeloma-experienced versus naive grafts (Figure 2A). To determine the functional relevance of expanded memory cell populations, we transplanted MM-bearing recipient mice with TCD-BM with or without CD44$^+$ or CD44$^-$ T cells from a myeloma-experienced donor (BMT$^+$-CD44$^+$ and BMT$^+$-CD44$^-$, respectively). We observed markedly improved myeloma control in recipients of BMT$^+$-CD44$^+$ T cells compared with recipients of BMT$^+$-CD44$^-$ T cells (Figure 2B), confirming the idea that memory T cells in the donor graft are the major effectors of myeloma control after BMT with myeloma-experienced donor T cells. Interestingly, BMT$^+$-CD44$^-$ T cell recipients had improved survival compared with the TCD-BMT group, demonstrating that myeloma-specific priming of naive donor T cells is also an operative immunological mechanism after BMT.

To further explore the role of preexisting donor myeloma–specific immunity, we phenotyped donor T cells in the BM of recipients 2 weeks after BMT with myeloma-experienced donor T cells. We noted a significant increase in CD8$^+$, but not CD4$^+$, T cells in recipients of BMT$^+$-CD44$^+$ T cells compared with those that received BMT$^+$-CD44$^-$ T cells, with expansion of CD8$^+$ T effector memory/effector ($T_{EM/EFF}$) cells in particular at this early time point (Figure 2C). Furthermore, this was unique to the BM, as CD8$^+$ T cell numbers were equivalent in the spleen (Supplemental Figure 4). These changes in CD8$^+$ $T_{EM/EFF}$ cell numbers were associated with an increase in the number of activated (DNAM-1$^+$PD-1$^+$) CD8$^+$ T cells (15) and a concomitant increase in exhausted (DNAM-1$^-$PD-1$^+$TIM-3$^+$) CD8$^+$ T cells (16, 17) in recipients of BMT$^+$-CD44$^+$ T cells (Figure 2D). These data indicate that antimyeloma responses may be amenable to further augmenta-

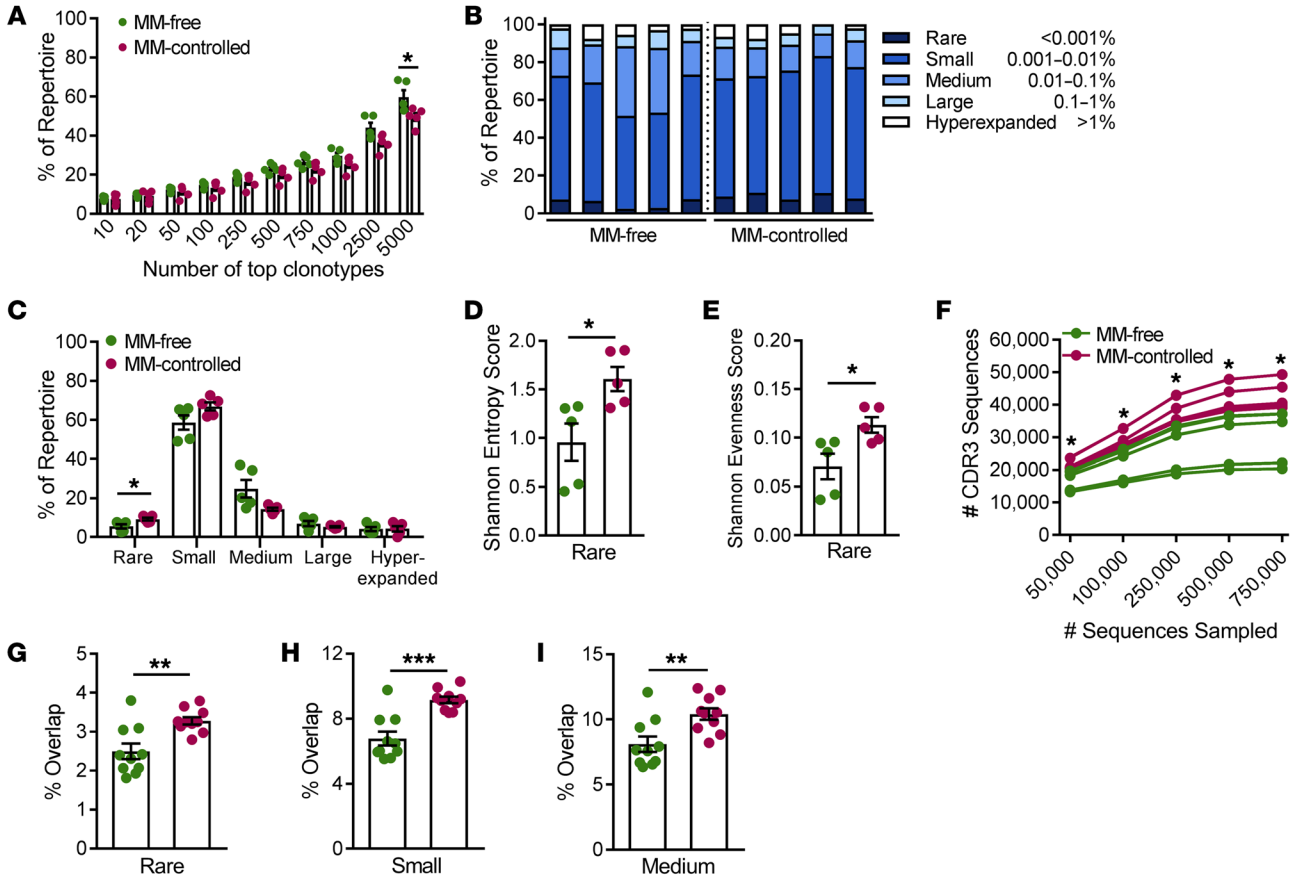

Figure 4. Adoptively transferred CD8⁺ T cells increase TCRβ repertoire diversity in Vk*MYC nonprogressor mice and exhibit strong clonotypic overlap. Adoptively transferred CD8⁺ T cells (CD45.2) were purified from the spleens of Vk12653-bearing mice with controlled disease (MM-controlled) and MM-free transplant control mice (MM-free) for TCRβ deep sequencing (n = 5 per group). (**A**) Percentage of the TCRβ repertoire based on the frequency of increasing numbers of clonotypes. (**B** and **C**) Distribution of rare, small, medium, large and hyperexpanded clonotypes in the TCRβ repertoire. (**D**) Entropy and (**E**) evenness of the TCRβ repertoire in rare clonotypes. (**F**) Total unique CDR3 sequences identified in 50,000, 100,000, 250,000, 500,000, and 750,000 sampled sequences. Residue-identical TCRβ clonotype overlap in (**G**) rare, (**H**) small, and (**I**) medium T cell subsets (n = 5 pairs of mice in each cohort). Data represent the mean ± SEM. *P < 0.05, ** P < 0.01, and ***P < 0.001, by unpaired t test.

tion by immune checkpoint blockade after BMT with myeloma-experienced donor T cells. Importantly, donor T cells from BMT⁺-CD44⁺ grafts, the majority of which were CD8⁺, could be recovered in recipient BM more than 100 days after BMT⁺ (Figure 2E). The CD8⁺ T cell population included comparable proportions of T_{CM} and $T_{EM/EFF}$ cells (Figure 2F), suggesting a contraction of the early $T_{EM/EFF}$ expansion to maintain a long-term memory cell population, similar to that seen in acute viral infection (17, 18).

BMT with T cells from naive donors generates myeloma-specific T cell memory. To determine whether T cell–mediated control of myeloma, generated after BMT by priming naive T cells, was antigen specific and could be transferred to secondary recipients, we adoptively transferred T cells from BMT recipients with long-term control of disease (>120 days of progression-free survival; MM-experienced [MM-exp]). Secondary MM-bearing mice that received MM-exp T cells had very limited myeloma progression relative to the recipients of naive T cells (Figure 3A). Furthermore, late after transplantation, the recipients of MM-exp T cells had a significantly increased frequency of CD8⁺ T_{CM} cells in the BM compared with recipients of naive T cell grafts (Figure 3B). We observed no change in the frequency of T_{CM} cells in BM CD4⁺ T cells or in the spleen (Supplemental Figure 5). Additionally, we detected an increased frequency of antigen-experienced CD122⁺ T cells (19) within the CD8⁺ T_{CM} population in recipients of MM-exp T cell grafts compared with naive grafts (Figure 3C). These data further support the idea that expansion of a potentially antigen-specific, memory CD8⁺ T cell population controls myeloma progression. To explore this hypothesis, secondary recipient mice were injected with Vk12653 or Vk12598 myeloma cells and transplanted with TCD-BM and either T cells primed against Vk12653 or naive T cells. Mice bearing Vk12653 myeloma that were transplanted with T cells primed against the same clone had better survival rates than did recipients of naive T cells (Figure 3D). However, when recipients bearing Vk12598 were transplanted with T cells primed against Vk12653, we found that myeloma control was equivalent to that of recipients of naive T cells (Figure 3D), suggesting that T cell–mediated control of myeloma after BMT is indeed myeloma cell clone specific. Interestingly, when MM-exp CD8⁺ T cells were transferred with naive CD4⁺ T cells, the secondary recipients had reduced M-band levels 6 weeks after BMT compared with naive control T cells (Figure 3E). However, we found that significant protection was not conferred by MM-exp CD4⁺ T cells transferred

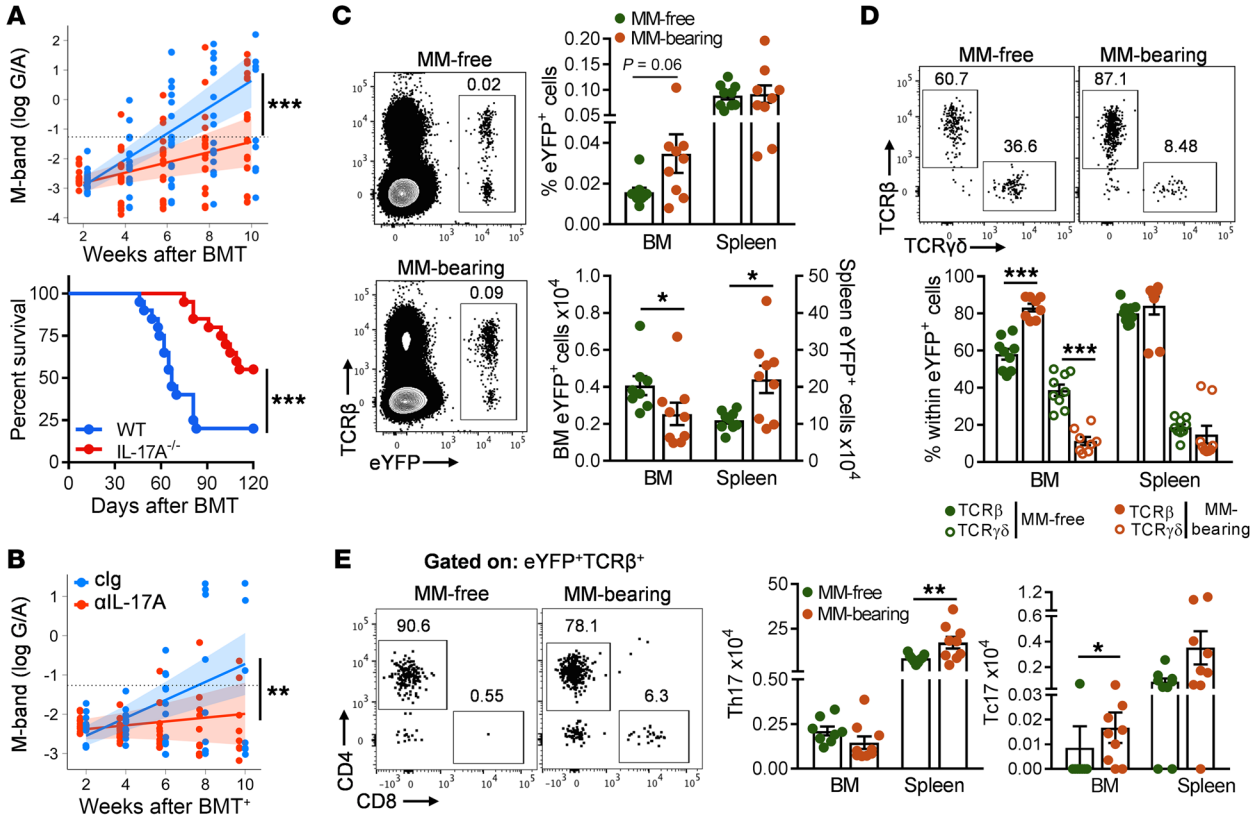

Figure 5. Donor-derived IL-17A promotes myeloma relapse after BMT. (**A**) Tumor burden, quantified and modeled using M-band levels as described, and survival in MM-bearing recipients transplanted with BM and T cells from WT or IL-17A–deficient (IL-17A$^{-/-}$) donors (n = 20 combined from 4 experiments). (**B**) M-band of MM-bearing BMT$^+$ with myeloma-experienced donors that were treated twice a week with 150 μg i.p of an IL-17A–blocking Ab or isotype control (clg) from day 0 to week 6 after BMT$^+$ (n = 12–13 combined from 2 experiments). (**C**–**E**) MM-free and MM-bearing recipient mice were transplanted with BM and T cells from IL-17A^{Cre}Rosa26eYFP donors. eYFP$^+$ cells were analyzed in BM (femur) and spleens 6 weeks after BMT. Representative dot plot (concatenated BM) and (**C**) total eYFP$^+$ frequency and numbers, (**D**) frequency of TCRγδ$^+$ and TCRβ$^+$ cells within the eYFP$^+$ cell population, and (**E**) total numbers of Th17 (eYFP$^+$ TCRβ$^+$CD4$^+$) and Tc17 (eYFP$^+$TCRβ$^+$CD8$^+$) cells (n = 9 combined from 2 experiments). Data represent the mean ± SEM. *P < 0.05, **P < 0.01, and ***P < 0.001, by log-rank test for survival and Mann-Whitney U test for numerical values.

with naive CD8$^+$ T cells compared with recipients of naive control T cells. These data suggest that CD8$^+$ T cells provide the major myeloma-specific immune memory after BMT.

In order to further characterize the generation of T cell–dependent myeloma control after BMT, we performed T cell receptor β (TCRβ) deep sequencing of donor CD8$^+$ T cells from mice that had controlled MM over the long term (MM-controlled) or from MM-free transplant controls (MM-free). The focus on CD8$^+$ T cells after BMT was based on the relatively high expression of MHC-I versus MHC-II on myeloma cells (Supplemental Figure 1B), the ability of CD8$^+$ T cells to contribute to myeloma immunity at steady state (20), and the necessity of MM-exp CD8$^+$ T cells to transfer protection to secondary recipients after BMT (Figure 3E). TCR sequencing revealed a distinct repertoire structure in MM-controlled mice compared with MM-free controls. MM-free mice exhibited more clonality in the most abundant clonotypes, which was significant when sampling the top 5,000 clonotypes (Figure 4A). This difference in repertoire composition was further validated when partitioning the CD8$^+$ T cell repertoire into rare, small, medium, large, and hyperexpanded clonotypes. MM-controlled mice had significantly more of the total repertoire invested in rare clonotypes and a similar trend for small clonotypes (Figure 4, B and C). In MM-controlled mice, this T cell repertoire subset also exhibited increased diversity, as seen by an increased Shannon entropy score (Figure 4D) and decreased clonality, as seen by an increased evenness score (Figure 4E). Additionally, the number of unique clonotypes was consistently increased in MM-controlled mice over a 50,000–750,000 sequence sampling analysis (Figure 4F), and differences in TCR gene usage were also observed, with a significant bias toward mTRBV12-1, mTRBV23, and mTRBV30 (Supplemental Table 1). We observed no overt differences in TRBJ usage or CDR3 length between MM-controlled and MM-free mice (data not shown). Importantly, we observed significantly higher TCR overlap between MM-controlled mice compared with MM-free mice when analyzing the rare, small, and medium repertoires (Figure 4, G–I). Given that the MHC-I–restricted T cell response against tumor antigens is often biased by TCRβ chain variable (TRBV) usage and/or involves residue-identical (public) TCR deployment (reviewed in ref. 21), these data suggest that a significant number of CD8$^+$ T cells in MM-controlled mice had expanded against Vk12653 myeloma antigen(s).

IL-17A subverts myeloma-immune equilibrium after BMT. The fact that CD4$^+$ T cells controlled myeloma despite its very low expression of MHC-II suggests that these CD4$^+$ T cells may act

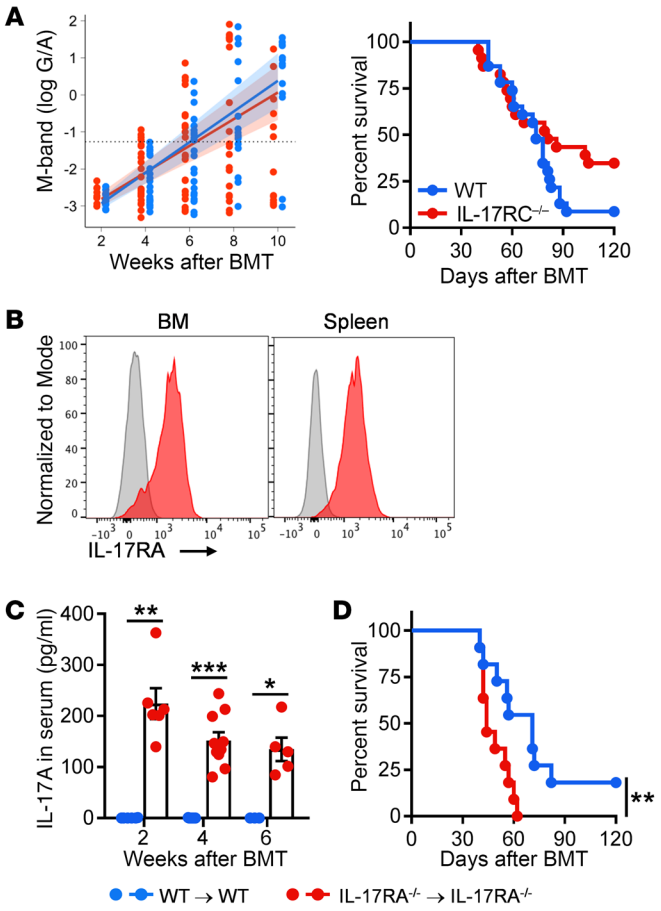

Figure 6. Donor-derived IL-17A acts directly on myeloma cells to promote progression. (**A**) Tumor burden, quantified and modeled using M-band levels as described, and survival of MM-bearing recipients transplanted with BM and T cells from B6.WT or B6.IL-17 receptor subunit C–deficient (IL-17RC$^{-/-}$) donors (n = 23 combined from 3 experiments). (**B**) IL-17RA (red, with isotype in gray) expression on VK12653 myeloma cells harvested from the BM and spleens of MM-bearing mice. (**C** and **D**) MM-bearing WT recipient mice were transplanted with WT grafts, while MM-bearing IL-17RA$^{-/-}$ mice were transplanted with IL-17RA$^{-/-}$ grafts. All recipient mice were cohoused for 4 weeks prior to BMT. (**C**) Serum levels of IL-17A (week 2, n = 6; week 4, n = 9–10; week 6, n = 3–5) and (**D**) survival (n = 11 combined from 2 experiments). Data represent the mean ± SEM. *P < 0.05, **P < 0.01, and ***P < 0.001, by log-rank test for survival data and Mann-Whitney U test for numerical values.

via the release of soluble factors during T cell differentiation, independently of cognate TCR–MHC-II interactions with myeloma targets. We first investigated whether Th17 immunity played a role in myeloma relapse after BMT, since IL-17 has been suggested to be involved in myeloma progression (22, 23). We found that IL-17A deficiency in donor grafts significantly improved myeloma control after BMT (Figure 5A). We used the BMT model to address this, as the growth of myeloma was modified in a number of naive knockout donor strains, preventing the use of these mice as myeloma-experienced donors. Nevertheless, inhibition of IL-17A with a mAb also improved myeloma control after BMT from myeloma-experienced donors (Figure 5B). Deficiency of donor-derived IL-6, a cytokine known to promote Th17 differentiation (24) and a known growth factor for myeloma (25), also improved myeloma control after BMT (Supplemental Figure 6A). However, this effect of IL-6 was probably due to direct effects on myeloma growth, as Th17 differentiation remained largely intact (Supplemental Figure 6B), given the known ability of recipient cells to generate IL-6 after transplantation and drive Th17 differentiation (26). Indeed, the importance of recipient-derived IL-6 was confirmed by the inability of myeloma to progress when both the recipient and donor were IL-6 deficient (Supplemental Figure 6C). In concert, Vk*MYC myeloma cells expressed the IL-6 receptor and the coreceptor Gp130 (Supplemental Figure 6D) and phosphorylated STAT3 in response to IL-6 (Supplemental Figure 6E), consistent with expression of the IL-6 signaling complex on primary myeloma patients' samples (27). To determine whether myeloma itself could influence type 17 polarization, we used IL-17A fate-mapped reporter donors (IL-17^{Cre}Rosa26eYFP), in which enhanced YFP (eYFP) is permanently expressed in cells that have ever produced IL-17A, regardless of continued IL-17A gene transcription (28). While we noted a trend toward increased eYFP$^+$ cell frequency in the BM of MM-bearing mice (P = 0.06), we noted a small decrease in the overall number due to impaired hematopoiesis in the MM-bearing mice (Figure 5C). We detected no change in the frequency of eYFP$^+$ cells in the spleen; however, eYFP$^+$ cell numbers were significantly increased as a result of splenomegaly in the MM-bearing-mice (Figure 5C). Within the eYFP$^+$ cell population in mice bearing myeloma, an expansion of TCRβ$^+$ relative to TCRγδ$^+$ T cells was seen in the BM (Figure 5D). The majority of eYFP$^+$TCRβ$^+$ cells were CD4$^+$ T cells (Th17), although myeloma also induced a small but significant expansion of CD8$^+$ T cells (Tc17) (Figure 5E). We next investigated cytokine production by eYFP$^+$ cells in the spleens of MM-bearing and MM-free mice after BMT. As expected, we found that the majority of eYFP$^+$ cells had significant IL-17A production, and similar levels of TNF, GM-CSF, IFN-γ, and IL-22 were also seen in MM-free and MM-bearing mice (Supplemental Figure 7). Taken together, these data suggest that, although myeloma has limited influence on donor Th17 differentiation per se, donor IL-17A secretion is demonstrable after BMT and is sufficient to promote myeloma progression.

Donor-derived IL-17A acts directly on myeloma cells to promote progression after BMT. Given the observed role of donor-derived IL-17A in subverting myeloma-immune equilibrium after BMT, we investigated whether donor or recipient compartments were responding to IL-17A to mediate this effect. We thus transplanted grafts that were deficient in a critical IL-17A signaling receptor subunit (IL-17RC$^{-/-}$) and noted myeloma progression similar to that seen when donor grafts were WT (Figure 6A). Interestingly, there was a small but nonsignificant increase in the number of recipients of IL-17RC$^{-/-}$ grafts that entered the plateau phase late after BMT. Nonetheless, these data clearly demonstrate that IL-17A was acting directly on the recipient compartment, putatively BM stroma or myeloma itself, since the latter also expressed high levels of the IL-17A receptor (Figure 6B). To distinguish these possibilities, we used IL-17R subunit A–deficient (IL-17RA$^{-/-}$) mice as both recipients and donors, such that IL-17A could only signal in myeloma cells. Given the known

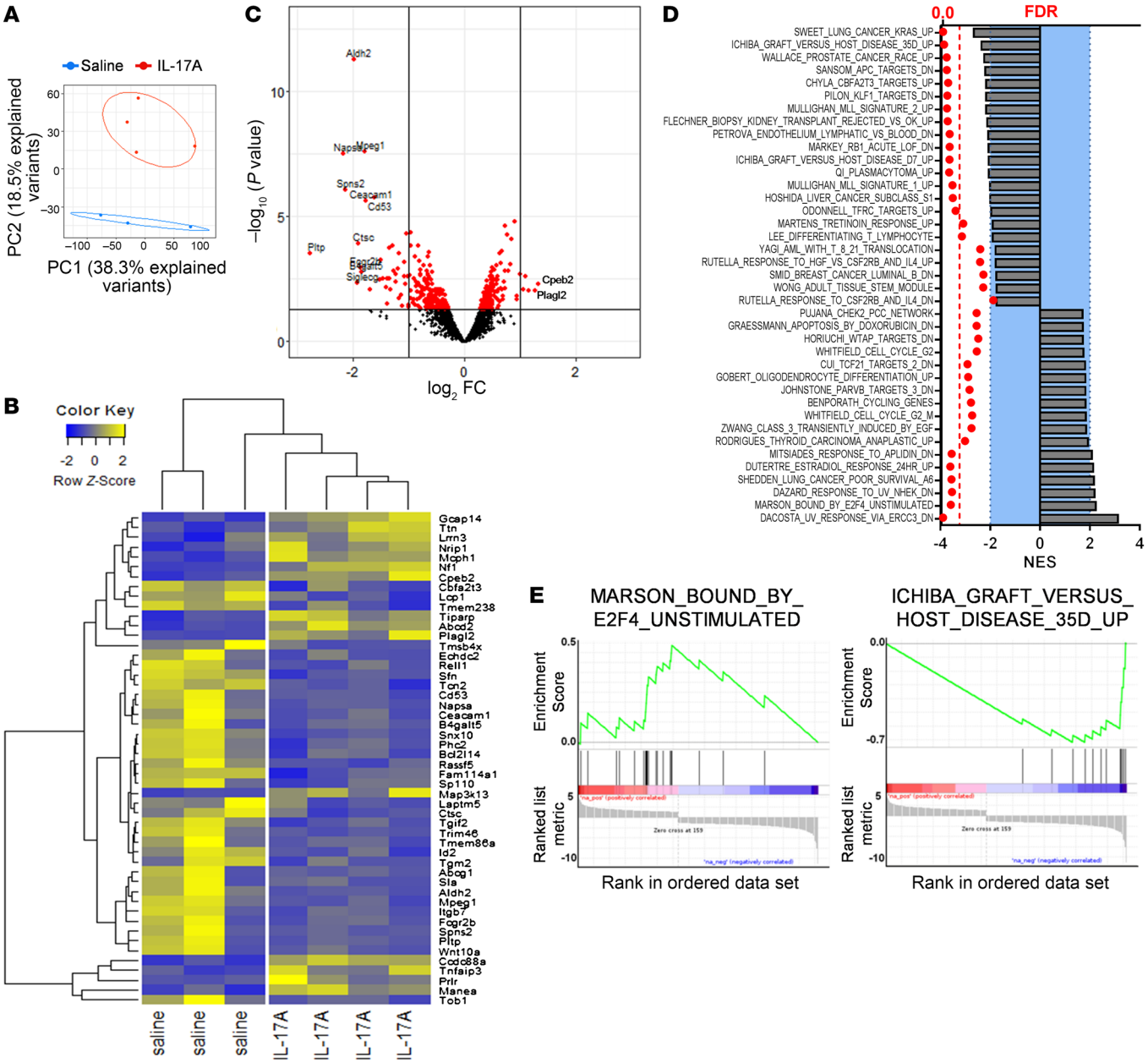

Figure 7. Gene expression profiling of IL-17A–treated Vk*MYC myeloma. Splenic Vk12653 myeloma cells were harvested from Rag$\gamma c^{-/-}$ mice treated with IL-17A or saline, and RNA-Seq was performed. (**A**) Principal component analysis (PCA) plot of the replicate samples from IL-17A–treated (n = 4) and saline-treated (n = 3) groups. (**B**) Heatmap of 50 genes and (**C**) volcano plot of genes that were differentially expressed between the IL-17A– and saline-treated groups. (**D** and **E**) GSEA of differentially expressed genes was determined by querying the MSigDB. (**D**) Summary of differentially expressed pathways. The red dotted line is drawn at a FDR of 0.05, and the shaded areas denote normalized enrichment scores (NES) between –2 and +2. (**E**) Enrichment plot for a set of genes with promoters bound by E2F4 and enrichment plot for genes involved in antigen processing and presentation and leukocyte migration and activation. $P < 0.05$, FDR <0.2; NES >1.75 and <1.75. The P value for a GSEA analysis was calculated using the Kolmogorov-Smirnov statistics comparing ranks of P values of genes in the gene set versus uniform distribution.

dysbiosis in these mice, all recipient mice were cohoused for 4 weeks prior to BMT to equilibrate their gastrointestinal microbiomes (29). In the absence of IL-17A signaling and subsequent consumption, systemic IL-17A levels were elevated in the IL-17RA$^{-/-}$ → IL-17RA$^{-/-}$ recipient mice (Figure 6C), and myeloma developed rapidly in these mice (Figure 6D), confirming that direct signaling to myeloma cells by IL-17A does in fact drive myeloma progression.

A role for IL-17A as a myeloma growth factor has not been examined after BMT, and so we next determined the effects of IL-17A signaling on myeloma cells in vivo. To limit contributions of endogenous T cell–derived IL-17A, we treated MM-bearing Rag2$\gamma c^{-/-}$ mice with exogenous recombinant mouse IL-17A or saline and collected myeloma cells thereafter for RNA-Seq. We detected clear differences in the transcriptome of myeloma cells exposed to IL-17A in vivo (Figure 7A). We identified 381

Table 1. Selected significantly altered genes (FDR <0.05) in Vk*MYC myeloma after treatment with IL-17A

Gene	Fold change (log)	FDR	Function/role
Decreased with IL-17A treatment			
Napsa	−2.18	9.4×10^{-05}	Protein metabolism
Spns2	−2.14	2.0×10^{-03}	Lymphocyte trafficking
Aldh2	−1.98	5.0×10^{-08}	Enzyme, oxidative pathway
Mpeg1	−1.78	9.4×10^{-05}	Membrane pore formation
Ceacam1	−1.77	3.6×10^{-03}	Adhesion molecule
Cd53	−1.62	3.4×10^{-03}	Regulation of cell growth and motility
Id2	−1.04	4.4×10^{-02}	Transcriptional regulator
Increased with IL-17A treatment			
Gcap14	0.728	2.7×10^{-02}	Cell proliferation and differentiation
Plagl2	0.768	4.4×10^{-02}	Transcriptional activator
Cpeb2	0.906	2.2×10^{-02}	Cell-cycle progression

differentially expressed genes with a *P* value of less than 0.05, of which 11 were significantly different after FDR correction (Figure 7, B and C, and Table 1). Interestingly, Plagl2, which was upregulated with IL-17A treatment, has been shown to promote cell proliferation in leukemia (30, 31), and Spns, which was downregulated with IL-17A treatment, has been shown to impair STAT3-mediated prosurvival pathways in lung cancer (32). Taken together, this suggests that IL-17A may promote the survival and proliferation of myeloma cells. To characterize the pathways affected in myeloma by IL-17A treatment, we queried up- and downregulated genes against the Molecular Signatures Database (MSigDB) (Figure 7D). Gene set enrichment analysis (GSEA) of the transcriptome of IL-17A–treated myeloma revealed 21 significantly altered pathways (FDR <0.05) including those involved in cell cycling, metabolism, proliferation, and migration. Of note, a set of genes with promoters bound by E2F4, which promotes proliferation in cancer cells (33), was upregulated in response to IL-17A (Figure 7E). Furthermore, genes related to antigen processing and presentation and leukocyte trafficking and activation (34) were downregulated in response to IL-17A (Figure 7E). Thus, donor-derived IL-17A drives intrinsic myeloma progression directly after BMT, independent of T cell immunity, highlighting IL-17A as a potential therapeutic target.

Donor IFN-γ secretion and signaling control myeloma after BMT and can be augmented by agonistic CD137 Ab treatment. Given the importance of Th1 immunity in tumor control, we next analyzed IFN-γ secretion by $CD8^+$ T cells after BMT in mice in which myeloma had relapsed (MM-relapsed) or was being controlled (MM-controlled) or in mice that were transplanted in the absence of myeloma altogether (MM-free). While IFN-γ production from $CD4^+$ T cells was unaffected by MM-relapse after BMT (data not shown), these mice had impaired IFN-γ secretion (Figure 8, A and B) and reduced total numbers of IFN-γ–secreting $CD8^+$ T cells relative to numbers in MM-controlled and MM-free mice (Figure 8C). In order to understand the functional consequences of this, we used IFN-γ–deficient (IFN-$\gamma^{-/-}$) and IFN-γ receptor–deficient (IFN-$\gamma R^{-/-}$) grafts in our transplant systems. Critically, recipients of both graft types rapidly developed myeloma, which indicated a crucial role for donor-derived IFN-γ generation and signaling in the immune equilibrium seen after BMT (Figure 8D).

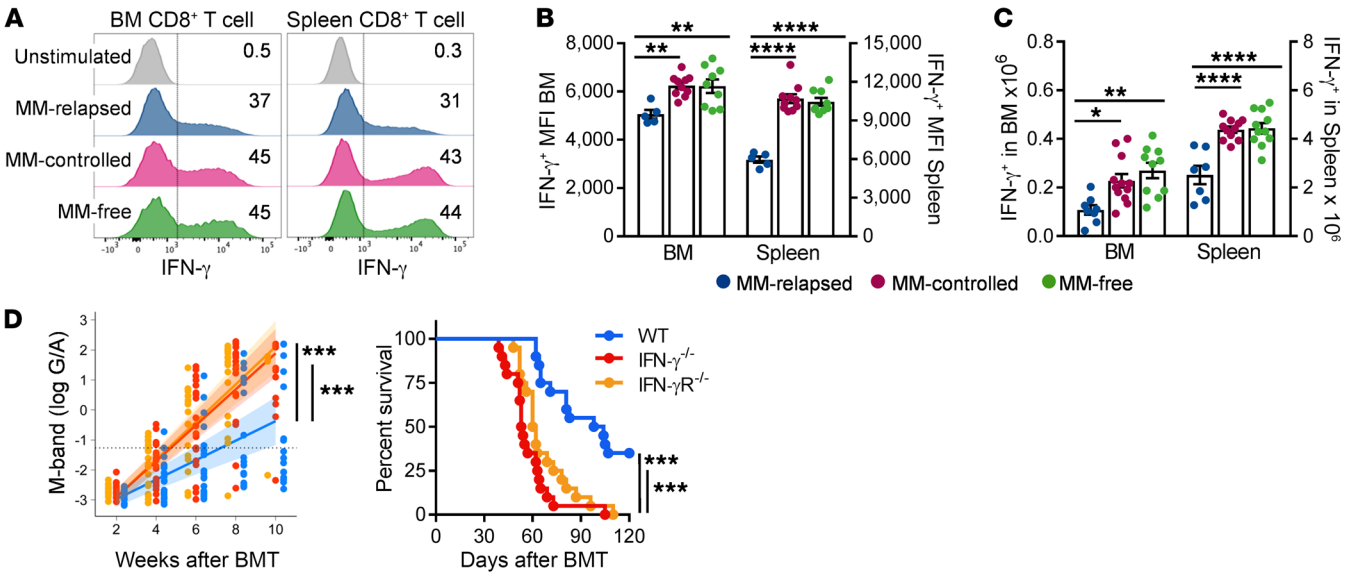

Figure 8. Immunological control of myeloma is IFN-γ dependent. (**A**–**C**) MM-bearing or MM-free B6.WT mice were transplanted as previously described, and IFN-γ production was determined ex vivo 8 weeks later. (**A**) Representative histograms, (**B**) geometric MFI, and (**C**) absolute numbers of IFN-γ–producing $CD8^+$ T cells in mice with active myeloma progression (MM-relapsed) or controlled disease (MM-controlled) and in transplant control mice (MM-free) (MFI, *n* = 5–10 from 2 experiments; absolute number, *n* = 7–12 combined from 3 experiments). (**D**) Tumor burden and survival of MM-bearing recipient mice transplanted with BM and T cells from B6.WT, B6.IFN-$\gamma^{-/-}$, or B6.IFN-$\gamma R^{-/-}$ donors (*n* = 20 combined from 4 experiments). Data represent the mean ± SEM. $^*P < 0.05$, $^{**}P < 0.01$, $^{***}P < 0.001$, and $^{****}P < 0.0001$, by log-rank test for survival data and Mann-Whitney *U* test for 2-sample and ANOVA for multiple-sample comparisons.

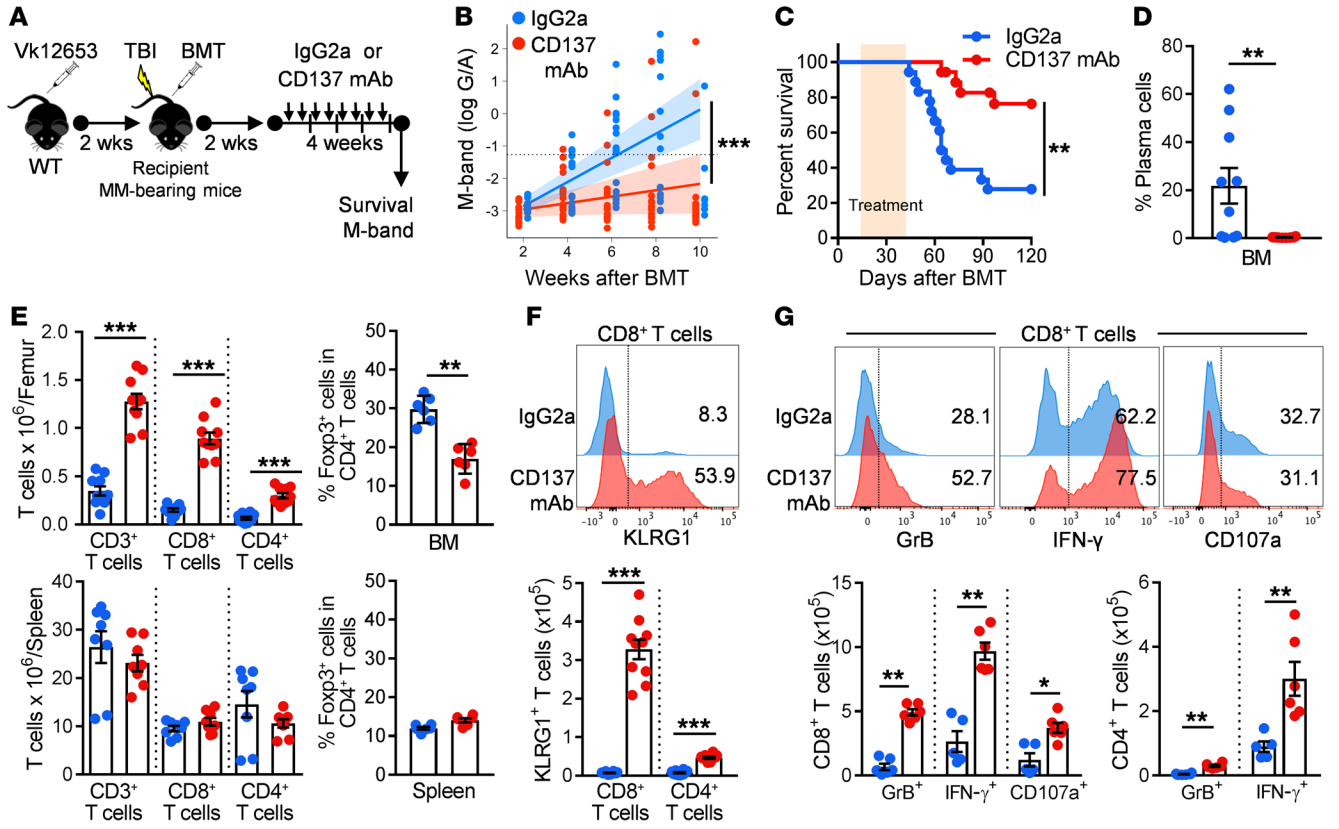

Figure 9. CD137 costimulation promotes long-term eradication of myeloma after BMT. MM-bearing recipient mice were transplanted with BM and T cells from B6.WT donors. Agonistic CD137 (clone 3H3) or a control mAb (IgG2a) was administered from week 2 to week 6 after BMT. (**A**) Illustration of experimental design. (**B**) Tumor burden, quantified using M-band levels as described, and (**C**) overall survival (n = 18 combined from 2 experiments). (**D**–**G**) BM and spleens were harvested after treatment ceased, and cells were analyzed using flow cytometry (n = 5–10 from 1 to 2 experiments). (**D**) Percentage of $CD138^+CD19^-$ myeloma cells in BM. (**E**) Absolute numbers of $CD3^+$, $CD8^+$, and $CD4^+$ T cells and frequency of $FoxP3^+$ within $CD4^+$ T cells in BM and spleens. (**F**) Representative histograms show KLRG1 expression in $CD8^+$ T cells and absolute numbers of $KLRG1^+$ cells within $CD8^+$ and $CD4^+$ T cells in BM. (**G**) Representative histograms show GrB, IFN-γ, and CD107a expression in $CD8^+$ T cells and graphs show absolute numbers of GrB^+, IFN-γ^+, and $CD107a^+CD8^+$ T cells and GrB^+ and IFN-γ^+CD4^+ T cells in BM. Data represent the mean ± SEM. $^*P < 0.05$, $^{**}P < 0.01$, and $^{***}P < 0.001$, by log-rank test for survival data and Mann-Whitney U test for numerical values.

The importance of Th1/Tc1 immunity in the control of myeloma led us to explore the ability of agents that might further expand this pathway. CD137 (4-IBB) agonists have proven effective in this regard and are entering clinical trials (20, 35). Thus, we administered a CD137 agonistic mAb for 4 weeks, commencing 2 weeks after transplantation, when myeloma was in a state of MRD (Figure 9A). This resulted in a dramatic improvement in myeloma control as demonstrated by reductions in M-band levels, improved survival, and complete eradication of myeloma from the BM (Figure 9, B–D). Importantly, CD137 agonist administration increased T cell numbers in BM, but not the spleen, while reducing the proportions of Tregs in the $CD4^+$ T cell compartment (Figure 9E). Finally, $CD8^+$ T_{EFF} cell frequency and function, as determined by KLRG1 (Figure 9F), granzyme B (GrB), and IFN-γ expression, were also increased in the BM (Figure 9G), consistent with the profound immune-driven control of myeloma. Similar effects of CD137 agonist administration were observed after BMT with myeloma-experienced donors, with decreased M-band, increased numbers of $CD8^+$ and $CD4^+$ T cells, and increased numbers of $KLRG1^+$, $Ki67^+$, GrB^+, $CD107a^+$, IFN-γ^+, and TNF^+CD8^+ T cells in the BM of Ab-treated recipients (Figure 10, A–C). However, this increase in $CD8^+$ T_{EFF} function was associated with an upregulation of PD-1 and TIM-3, which are early features of exhaustion that are most appreciable and defined by t-distributed stochastic neighbor embedding (t-SNE) analysis (Figure 10, D and E). Importantly, we found that exhaustion was not an irreversible phenotype, as determined by the absence of CD101 and CD38 coexpression (36) (Figure 10E). We thus reasoned that PD-1 inhibition would further augment the protective effect of CD137 agonists in MM-bearing BMT^+ recipients. In these experiments, we transplanted lower doses of donor T cells and started PD-1 inhibition treatment 10 days after CD137 administration (Figure 10F). This short-term PD-1 inhibition, late after BMT^+, had no effect on myeloma burden in isolation. Treatment with CD137 alone resulted in stabilization of myeloma burden, while disease burden in the isotype control group had progressed by 4 weeks after BMT^+. The mice treated with the combination of CD137 mAb and anti–PD-1 showed dramatic control of myeloma, and there was a reduction in myeloma burden from week 2 to week 4 after BMT^+, consistent with active antimyeloma immunity (Figure 10F). Thus, administration of CD137 agonists in combination with PD-1 blockade early after BMT, when IFN-γ and T cell–mediated immunological control have been initiated, represents an attractive approach to improve the depth and length of remission after transplantation.

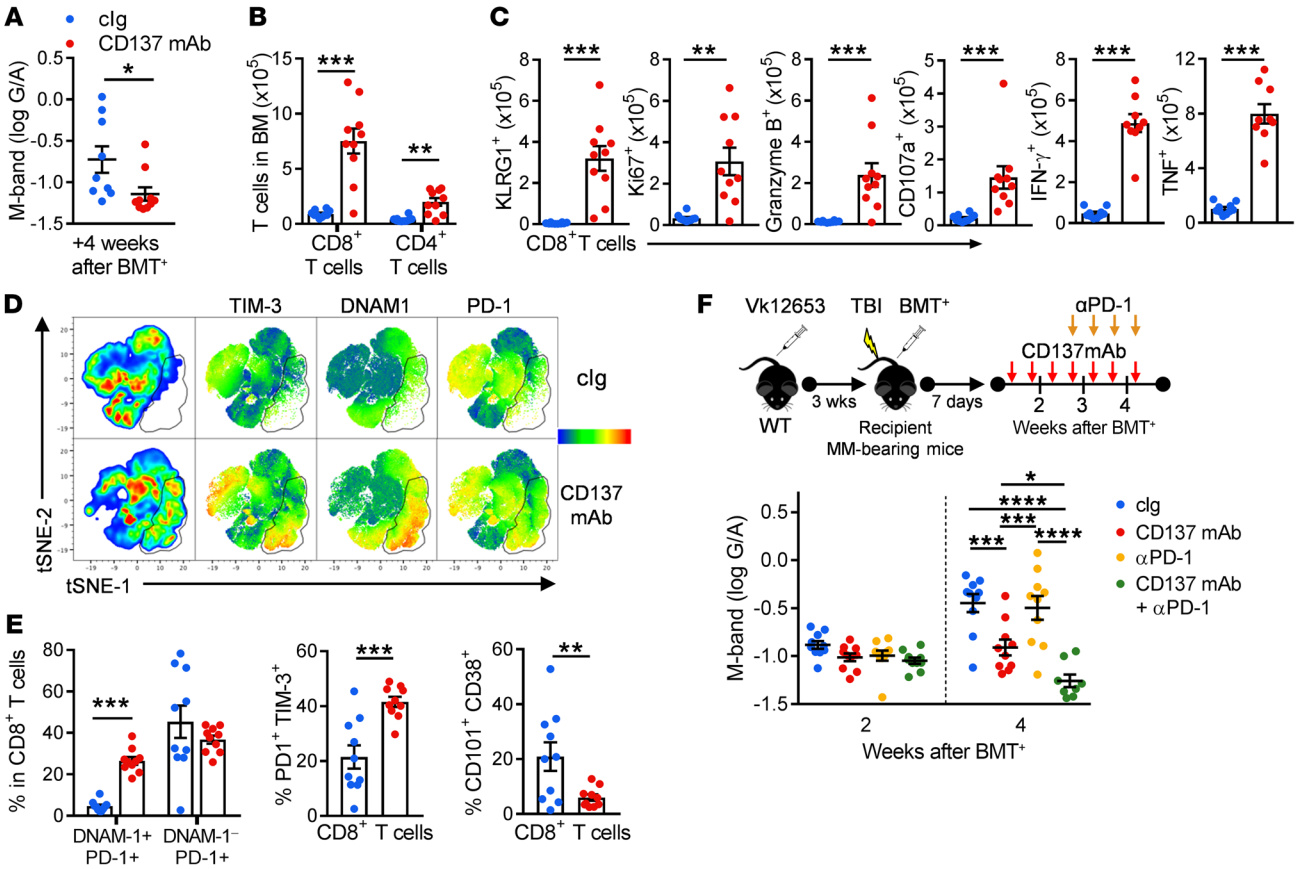

Figure 10. CD137 costimulation is augmented by PD-1 blockade after BMT with myeloma-experienced T cells. MM-bearing recipient mice were transplanted with naive TCD-BM and T cells from myeloma-experienced donors. Agonistic CD137 (clone 3H3) or a control mAb (IgG2a) was administered from week 1 to week 5 after BMT+. (**A**) Tumor burden, quantified using M-band levels as described (*n* = 10 combined from 2 experiments). (**B**–**F**) BM was harvested after treatment ceased, and cells were analyzed using flow cytometry (*n* = 8–10, from 1 experiment). (**B**) Absolute numbers of CD8+ T and CD4+ T cells in BM. (**C**) Absolute numbers of KLRG1+, Ki67+, GrB+, IFN-γ+, TNF+, and CD107a+CD8+ T cells in BM. (**D**) tSNE analysis and heatmaps of median CD8+ T cell exhaustion marker coexpression. (**E**) CD8+ T cell exhaustion marker quantification. (**F**) Experimental design and M-band levels of MM-bearing recipients transplanted with 1 × 10^6 myeloma-experienced T cells and 10 × 10^6 naive TCD-BM cells and treated with CD137 mAb alone (from day 7), anti–PD-1 alone (from day 17), CD137 mAb plus anti–PD-1, or isotype control (cIg). Data represent the mean ± SEM. **P* < 0.05, ***P* < 0.01, ****P* < 0.001, and *****P* < 0.0001, by Mann-Whitney *U* test for 2-sample and ANOVA for multiple-sample comparisons.

Discussion

Autologous SCT remains the standard consolidation treatment for patients with myeloma, and the development of strategies to increase the depth and duration of response remains a critical clinical objective. Here, we demonstrate a hitherto unappreciated and potent T cell–mediated process of immune control after transplantation that indicates the reestablishment of a state of myeloma-immune equilibrium. We show that this process involves clonotypic donor CD8+ T cell expansion and demonstrate T cell–mediated and antigen-specific myeloma control in secondary recipients. Importantly, Th17 differentiation impairs this process via the direct action of IL-17A on myeloma cells, while IFN-γ secretion and signaling in donor graft are critical for myeloma-specific immunity, which can be enhanced via CD137 costimulation.

Currently, there is clear but indirect evidence for immune-mediated control of myeloma. First, a cohort of patients who entered SCT while in CR achieved long-term survival thereafter (6), consistent with the immune control most commonly ascribed to allogeneic SCT (37). Second, while the progression of long-standing MGUS to active myeloma occurs within a landscape characterized by an accumulation of genetic defects (38), it is also consistent with (and not mutually exclusive to) the well-described characteristic of immunological tumor escape (39, 40). Finally, myeloma itself is associated with immune defects that may contribute to disease penetrance (41). To date, NK cells have been identified as key mediators of antimyeloma effects, especially following treatment with immunomodulatory drugs (IMiDs) (42–44). Expanded T cell populations bearing specific TCR-Vβ families, as assessed by flow cytometry, have been observed in myeloma patients with long-term control of disease (45, 46), and T cells from the BM of myeloma patients have been shown to respond to autologous tumor presented by dendritic cells in vitro (47, 48). However, these studies were performed in patients undergoing treatment with IMiDs, which are known to expand T cell clones (49), and it is unclear whether these changes in the T cell repertoire are generated in response to the myeloma or whether the T cells have myeloma-specific immunity. These clinical findings are, by nature, observational, and studies in the clinically relevant transplantation models described here are required to delineate true cause and effect.

In nontransplant preclinical models, T cells and NK cells have been implicated in myeloma progression in mice bearing Vk*MYC myeloma (20). Importantly, it cannot be assumed that immunity in nontransplant and transplant settings is equivalent. The generation of murine models of BMT can never completely recapitulate the entire clinical scenario. In particular, we cannot harvest marrow (or acquire adequate numbers of peripheral blood stem cells) from a mouse as a live procedure, but the value of working with inbred mice means this is not required to transplant immunologically identical grafts. Transplantation induces a profound inflammatory response, extensive myeloma cell death with subsequent MRD states, and a profound state of lymphodepletion, which is permissive of rapid proliferation and differentiation of transplanted donor T cells. To date, the beneficial outcomes of autologous SCT have been largely attributed to cytoreduction. Our study reveals a potent immunological aspect of transplantation, namely, the protective myeloma immunity driven by transplanted T cells rather than NK cells, either within the transplanted donor memory T cell fraction, or after transplantation within the naive T cell fraction. Importantly, the use of a MM-free transplant control in our TCR repertoire study provides critical evidence that changes in the T cell repertoire of mice with well-controlled disease were generated specifically in response to myeloma. Myeloma increased TCR diversity in the lower-abundance $CD8^+$ T cell compartment and significantly increased the overlap of shared clonotypes in the rare, small, and medium compartments. This is strong evidence for the generation of antigen-specific $CD8^+$ T cell memory for myeloma antigens in mice with controlled disease. Furthermore, adoptive transfer experiments using T cells from these mice showed that there is a functional memory response and that this response is Vk*MYC clone specific and is in fact conferred by $CD8^+$ T cells. Thus, we believe the present study provides new and definitive evidence for the establishment of antigen-specific, T cell–dependent myeloma control after BMT and shows the critical relationship to transplanted T cell subsets, the clinically important effect of prior exposure to myeloma, T cell clonality, and, finally, differentiation. Importantly, we also define methods to improve this process of active control after transplantation by driving IFN-γ–dependent T cell responses with αCD137-based immunotherapy and IL-17A inhibition.

In support of this concept of immunological control, we have recently demonstrated that myeloma progression after BMT is associated with $CD8^+$ T cell exhaustion and may be prevented by T cell Ig and ITIM domain (TIGIT) blockade (50). Together, these studies define an important new concept that SCT for myeloma is probably more than just cytoreduction and provide rational immune-based interventions that require testing, with the aim of improving post-BMT clinical outcomes for patients.

The role of T cell differentiation and cytokine production in myeloma control is unclear, and a consensus has not been reached, particularly regarding the role of Th17 differentiation. Th17 differentiation is driven by IL-6 signaling, which is supported by other cytokines (e.g., IL-21 and IL-23) (51). IL-6 is known to act as a myeloma growth factor and is dysregulated in patients undergoing transplantation (40, 52). Clinical studies have shown elevated levels of IL-17A in the sera of patients with myeloma (53), a finding that has been linked to angiogenesis (54). Paradoxically, then, Th17 differentiation has been reported as both unaffected (22) and reduced in patients with myeloma relative to healthy controls (55). Primary clinical myeloma samples are known to express the IL-17R (22), as does Vk*MYC myeloma, and myeloma is thus able to respond to IL-17A directly. Experiments culturing myeloma cell lines with exogenous IL-17A in vitro suggest that IL-17A may promote cell growth, however, attempts to address this in vivo have only been performed in immunocompromised mice with s.c. tumors (22). Additional studies suggest that myeloma itself produces IL-17A that acts on BM stromal cells to produce IL-6, raising the possibility that myeloma-derived IL-17A acts in a paracrine fashion (23). In contrast, we have shown that, after transplantation, IL-17A is produced by donor T cells and acts directly on myeloma cells, independent of effects on nonmalignant donor or host tissue. Importantly, we demonstrate that IL-17A signaling in myeloma results in significant prosurvival transcriptional activity, although we could not see amplification of IL-6 mRNA as part of this response. It should be noted that we have not excluded the possibility of an additional role for IL-17A secretion and paracrine signaling in MM and that the two mechanisms are not mutually exclusive.

The immunological control of most tumors has been defined as a Th/Tc1 process, in which IFN-γ secretion and signaling are pivotal (39, 40). Indeed, initial studies in vitro demonstrated that IFN-γ inhibits myeloma cell growth (56) and, in vivo, Vk*MYC myeloma results in accelerated lethality in IFN-$\gamma^{-/-}$ mice (20). Importantly, IFN-γ production by PBMCs appears similar in patients with various stages of MM and in healthy controls (57). Surprisingly, given the nature of the disease, IFN-γ production by T cells has not been well described in the BM tumor microenvironment of patients with MM. We observed that $CD8^+$ T cells from transplanted mice with progressive myeloma had impaired IFN-γ production, while it was unaffected in those with controlled myeloma. Consistent with this, agonistic CD137 mAb eradicated myeloma in the majority of transplanted animals by increasing Th1/Tc1 expansion, consistent with the known antitumor activity of IFN-γ in cancer models (20, 58–60). The antimyeloma activity of CD137 agonists has been reported in preclinical nontransplant settings (20, 60), and a phase I trial (NCT02252263) has recently been completed, however, no results have been reported to date. Importantly, our study suggests that CD137 agonists could be used in combination with autologous SCT to improve clinical outcomes. Furthermore, our data highlight the finding that a combination approach using CD137 agonists and PD-1 inhibition may further improve clinical outcomes after autologous SCT.

We believe our study has major implications for how myeloma might be optimally treated. First, clinical data, although retrospective and registry based, suggest that outcomes for myeloma after syngeneic transplantation are superior to those after autologous transplantation (61, 62). While this may theoretically reflect a benefit from using a graft free of contamination by myeloma cells, studies purging grafts to eliminate contamination have not improved outcomes (63–65), and gene-marking studies have not shown relapse to be derived from myeloma cell contamination within the graft, at least as a common event (66). More likely, then, the transplantation of a fully immunologically competent syngeneic graft is responsible for this effect, such that the transplanted immune system is free from any prior exposure to cytore-

ductive and immunosuppressive agents, a scenario that is replicated in our murine model, in which BM grafts were harvested from immunogenically identical but untreated donors. Additionally, the presence of preexisting myeloma-specific T cells in the memory compartment of myeloma-experienced donor grafts provides support for immunologically focused studies of induction regimens permissive of immune competence prior to stem cell collection, with a correlation to immunological and clinical outcomes thereafter. Second, preventing IL-17A signaling to myeloma cells could improve transplantation outcomes, and anti–IL-17A Abs are already available for the treatment of other inflammatory diseases (67–69). Finally, with the availability of multiple PD-1 inhibitors and 2 humanized agonistic CD137 mAbs, urelumab (Bristol-Myers Squibb, e.g., NCT02252263) and PF-05082566 (Pfizer), treatment with anti-CD137 and anti–PD-1 after autologous SCT, when in a state of MRD, could provide a novel means of improving immune-based cures for patients.

Methods

Mice. Female, 8- to 12-week-old C57BL/6 (B6.WT; CD45.2) and B6.Sjl. PTPRCA (CD45.1) mice were purchased from the Animal Resources Center (Perth, Western Australia, Australia). B6.45.1/45.2 mice and knockout mice on a B6 background: B6.IL-17RC$^{-/-}$ and B6.IL-17RA$^{-/-}$ (Amgen); B6.IL-17A$^{-/-}$ (provided by Y. Iwakura, The University of Tokyo, Tokyo, Japan); B6.IFN-γ$^{-/-}$ and B6.IFN-γR$^{-/-}$ (The Jackson Laboratory); and B6.Jα18$^{-/-}$ (Peter Mac [Peter MacCallum Cancer Centre], East Melbourne, Victoria, Australia); B6.IL-6$^{-/-}$ (provided by S. Alexander, University of Sydney, New South Wales, Australia); and reporter B6.IL-17^{Cre}Rosa26YFP (described in ref. 28) mice were bred in-house (QIMR Berghofer Medical Research Institute). NKp46^{Cre} Mcl1$^{fl/fl}$ (Mcl1$^{fl/fl}$ mice were generated by Nicholas Huntington [ref. 11]), TCRδ$^{-/-}$, and RAGγc$^{-/-}$ mice were produced in house. Mice were housed in sterilized microisolator cages and received acidified (pH 2.5), autoclaved water and normal chow. For cohousing experiments, mice were housed in large cages for 4 weeks prior to transplantation and for the duration of the experiment after transplantation.

Abs. The following Abs used in this study were purchased from BioLegend: FITC-conjugated Ab against I-A/I-E (M5/114.15.2); phycoerythrin-conjugated (PE-conjugated) Abs against CD155 (4.24.1), NKp46 (29A1.4), IL-22 (poly5164), CD45.1 (A20), and rat IgG2a isotype control; PE-Cy7–conjugated PD-1 (RMP1-30) and rat IgG2b Ab; Alexa Fluor 647–conjugated Abs against H-2D^{b} (KH95), CD101 (RM101), and CD226 (TX42.1); Alexa Fluor 700–conjugated Abs against CD45.2 (clone 104), Ki67 (clone 16A8), CD62L (clone MEL-14), and IL-17A (clone TC11-8H10.1); allophycocyanin-conjugated (APC-conjugated) Abs against PD-L1 (CD274, clone 10F.9G2), KLRG1 (clone 2F1), GrB (clone GB12), TNF (clone MP6-XT22), TCRβ (clone H57-597), and Syrian hamster IgG, mouse IgG1, and rat IgG2b isotype controls; APC-Cy7–conjugated Abs against CD19 (clone 6D5), CD38 (clone 90), and CD8 (clone 53-6.7); PerCpCy5.5-conjugated Abs against CD122 (clone TM-β1) and GM-CSF (clone MP1-22E9); brilliant violet 421–conjugated Abs against CD138 (clone 281-2), IFN-γ (clone XMG1.2), CD44 (clone IM7), PD-1 (clone 29F.1A12), γδ-TCR (clone GL3), and rat IgG1 isotype control; brilliant violet 605–conjugated Abs against CD90.2 (clone 53-2.1) and CD4 (clone RM4-5). PE-conjugated Abs against IL-17RA (CD217, clone PAJ-17R) and TIM3 (clone RMT3-23) and PE-Cy–conjugated Ab against CD126 (IL-6R, clone D77ISA7) were purchased from eBioscience. PerCp-Cy5.5-conjugated Ab against CD8 (clone 53-6.7); PE-conjugated Ab against STAT3 (4/0-STAT3); and violet 450–conjugated Abs against CD107a (clone 1D4B) and rat IgG2a isotype control were purchased from BD Biosciences. PE-conjugated Ab against Gp130 (clone 125623) was purchased from R&D Systems. FITC-conjugated Ab against CD4 (clone GK1.5) was produced in house from hybridoma supernatant.

*Preclinical models of BMT using recipients bearing Vk*MYC myeloma*. Vk*MYC myeloma clones Vk12653 and Vk12598, which originate from Vk*MYC-transgenic mice and produce diverse monoclonal paraprotein (9), were provided by Marta Chesi (Mayo Clinic, Scottsdale, Arizona, USA). For subsequent experiments, myeloma cell clones were propagated in house in B6.WT and RAGγc$^{-/-}$ mice, respectively. Transplantable VK12653 and Vk12598 myeloma cell clones have been shown to have immunological outcomes similar to those of spontaneous-onset myeloma in Vk*MYC-transgenic mice (70). Recipient mice (hereafter referred to as MM-bearing mice) were injected i.v. with Vk*MYC myeloma cells 14 days prior to BMT and 21 days prior to BMT^{+} (1×10^{6} CD138^{+}CD19^{-} cells; Vk12653, unless otherwise stated). MM-bearing recipient mice were transplanted as described previously (71). In brief, on day 1, recipient mice received 1,000 cGy total body irradiation (TBI) (^{137}Cs source at 81 cGy/min), and on day 0, they transplanted with 10×10^{6} BM or T cell–depleted BM (TCD-BM) from B6.WT or transgenic (on a B6 background) donors with or without 5×10^{6} purified splenic CD3^{+} T cells (purity >80%; using magnetic bead depletion) for BMT or 5×10^{6} sorted CD3^{+} T cells (purity >99%) from donors from the concurrent recipient cohort for BMT^{+}. BM was depleted of T cells (TCD) using an Ab master mix against CD4, CD8, and CD90.2 and rabbit complement (Cedarlane Laboratories Ltd.) as described previously (72). Purified myeloma-experienced splenic CD3^{+} T cells from CD45.1/CD45.2 mice were stained with CD44 and CD62L and sorted via flow cytometry for BMT^{+} experiments with CD44^{+} and CD44^{-} T cell grafts. Recipients were bled every 2 weeks, and serum samples were analyzed using a Sebia Hydrasys serum protein electrophoresis system to quantify paraprotein as a G/A ratio (referred to as M-band), as previously described (73). Transplanted mice were monitored daily, up to 120 days, and sacrificed when clinical scores reached 6 or higher (described in ref. 74) or hind limb paralysis occurred. Anti-CD4–depleting Abs (GK1.5, purified from hybridoma supernatants, 500 μg/mouse, i.p., on day 0 and then 250 μg/mouse, i.p., thereafter) or anti-CD8–depleting Abs (53.5.8, purified from hybridoma supernatants, 150 μg/mouse, i.p.) were administered once a week from day 0 until 8 weeks after BMT. IL-17A mAb (M210, murinized form, Amgen) was administered twice a week for 6 weeks after BMT^{+} from day 0 (150 μg/mouse, i.p.). Agonistic CD137 mAb (clone 3H3, Bio X Cell) or control rat IgG2a Ab (provided by MJS) was administrated twice weekly from weeks 2 to 6 after BMT or from weeks 1 to 5 after BMT^{+} (100 μg/mouse, i.p.). The myeloma-experienced T cell dose was reduced to 1×10^{6} cells for the CD137 and anti–PD-1 combination experiment. Anti–PD-1 (RMP1-14, Bio X Cell) or rat IgG2a (Mac4, purified from hybridoma supernatants) was administered twice weekly with CD137 from day 17 to day 28 (100 μg/mouse, i.p.).

Adoptive transfer. Secondary recipient mice were injected with either Vk12598 or Vk12653 myeloma cells and transplanted with 10×10^{6} TCD-BM (naive B6.WT) and 5×10^{6} CD3^{+} T cells or 2×10^{6} CD4^{+} and 2×10^{6} CD8^{+} T cells primed against Vk12653 or naive T cells (B6.WT). CD3^{+} T cells were isolated using magnetic bead depletion, and

$CD4^+$ and $CD8^+$ T cells were sorted via flow cytometry (purity >98%) from splenocytes and lymph nodes of primary transplanted MM-bearing recipients with long-term control of disease (>120 days after BMT progression-free survival) or naive controls. Secondary recipients were sacrificed 120 days after BMT.

Cell preparation, phenotyping, and flow cytometric analysis. Depending on the experimental design, recipient mice were sacrificed at weeks 2–8 after BMT, and cells from BM and spleen were collected. For phenotype analysis, freshly isolated cells were stained with Abs and analyzed by multicolor flow cytometry. For intracellular cytokine staining, the collected cells were stimulated with PMA (5 μg/ml) and ionomycin (50 μg/ml) (Sigma-Aldrich) for 4 hours at 37°C with brefeldin A (BioLegend), which was included during the last 3 hours of culture. Cells were surfaced labeled, fixed, and permeabilized using the Cytofix/Cytoperm Kit (BD Biosciences), followed by staining with cytokine-specific Abs. To measure degranulation, based on CD107a expression, cells were stimulated with PMA and ionomycin in the presence of brefeldin A, monensin (BioLegend), and V450-conjugated CD107a Ab (BD Biosciences) for 5 hours at 37°C. To measure phosphorylated STAT3 levels, BM cells were collected from Vk12653-bearing mice and stimulated with recombinant mouse IL-6 (50 ng/ml for 15 minutes; BioLegend) or were unstimulated control BM cells. Cells were fixed and permeabilized and analyzed via flow cytometry. All samples were acquired on a BD LSR Fortessa (BD Biosciences), and cell population frequencies and protein expression were analyzed using FlowJo software, version 10. Dimensionality reduction was performed via t-SNE analysis of $CD90.2^+CD8^+$ lymphocytes downsampled (5,000 cells) and pooled across all experimental groups (n = 10 mice/group). Population clustering based on exhaustion/activation marker expression (CD69, TIGIT, TIM-3, DNAM-1, CD101, CD38, PD-1) was performed over 1,000 iterations with a perplexity of 30 using FlowJo software, and heatmaps of individual marker expression overlaid onto t-SNE plots were generated (blue = low, red = high). Manual gating was performed to highlight coexpression of exhaustion markers as shown.

Serum IL-17A detection. Serum IL-17A was detected using an Enhanced Sensitivity Cytometric Bead Array Kit (BD Biosciences) according to the manufacturer's instructions. Samples were acquired on a BD LSR Fortessa and analyzed using FCAP Array Software (BD Biosciences).

Exome sequencing, TCR, and RNA-Seq methods are described in the Supplemental Methods.

Statistics. Survival curves were plotted using Kaplan-Meier estimates and compared by log-rank (Mantel-Cox) test. Differences between TCR repertories were calculated by t test, and all other numerical variables were compared by 2-tailed Mann-Whitney U test for 2-sample and ANOVA for multiple-sample comparisons. Data are presented as the mean ± SEM, and a P value of less than 0.05 was considered significant. Tumor growth was modeled longitudinally using mixed-effects models with random intercepts and log M-band as the dependent variable. The independent variables were treatment group and time plus interaction terms. To test for differences in the rate of change of log M-band, least squares means contrasts were performed on the treatment groups. All contrasts were adjusted for multiple comparisons using Tukey's honestly significant difference (HSD). The M-band at which mice inevitably progressed was empirically estimated. This estimate was derived by considering mice longitudinally and applying a linear classifier for "progressed" and "not progressed" at each follow-up point. The M-band and follow-up point that maximized the Youden criteria empirically was chosen as the optimal cutpoint. This optimal cutpoint was further internally cross-validated. Across all mice, the optimal M-band for determining progression was 0.282, with sensitivity and specificity of approximately 90% each.

Study approval. All animal procedures were performed in accordance with protocols approved by the IACUC of the QIMR Berghofer Medical Research Institute.

Author contributions

SV and SAM designed, performed, and analyzed experiments and wrote the manuscript. DS conducted statistical analyses and provided modeling. KHG, TSW, ALP, PAJ, and PM analyzed and interpreted data. RDK and KRL performed experiments. AV and PZ performed experiments and provided experimental advice. CG, KAM, NDH, NW, MC, JJM, and MJS provided essential reagents and/or discussion and experimental advice. GRH conceived and designed experiments and wrote the manuscript.

Acknowledgments

This work was supported by research grants from the Cancer Council Queensland and the National Health and Medical Research Council (NHMRC). KAM is a Queensland Health Junior Clinical Research Fellow. CG is supported by a National Health and Medical Research Council (NHMRC) of Australia Early Career Fellowship (1107417) and a PdCCRS grant financed by Cancer Australia, Cure Cancer Australia, and Can Too (1122183). MJS is a NHMRC Senior Principal Research Fellow. GRH is a NHMRC Senior Principal Research Fellow and has received funding from Roche for clinical trials of IL-6 inhibition in transplantation. We acknowledge the assistance of the members of the Flow Cytometry and Imaging facility at QIMR Berghofer, particularly, Paula Hall, Michael Rist, and Grace Chojnowski. We thank Leif Bergsagel (Mayo Clinic, Phoenix, Arizona, USA) for reviewing the exome-sequencing data.

Address correspondence to: Geoffrey Hill, Fred Hutchinson Cancer Research Center, 1100 Fairview Avenue N, Seattle, Washington 98109, USA. Phone: 206.667.3324; Email: grhill@fredhutch.org. Or to: Slavica Vuckovic, Institute of Haematology, Royal Prince Alfred Hospital, Missenden Road, Camperdown, NSW, 2050, Australia. Phone: 61.2.95158483; Email: Slavica.Vuckovic@health.nsw.gov.au.

1. Morgan GJ, Walker BA, Davies FE. The genetic architecture of multiple myeloma. *Nat Rev Cancer*. 2012;12(5):335–348.
2. Cavo M, et al. Bortezomib with thalidomide plus dexamethasone compared with thalidomide plus dexamethasone as induction therapy before, and consolidation therapy after, double autologous stem-cell transplantation in newly diagnosed multiple myeloma: a randomised phase 3 study. *Lancet*. 2010;376(9758):2075–2085.
3. Moreau P, Avet-Loiseau H, Harousseau JL, Attal M. Current trends in autologous stem-cell transplantation for myeloma in the era of novel therapies. *J Clin Oncol*. 2011;29(14):1898–1906.
4. Attal M, et al. A prospective, randomized trial of autologous bone marrow transplantation and chemotherapy in multiple myeloma. Intergroupe Français du Myélome. *N Engl J Med*.

1996;335(2):91–97.
5. Child JA, et al. High-dose chemotherapy with hematopoietic stem-cell rescue for multiple myeloma. *N Engl J Med*. 2003;348(19):1875–1883.
6. Martinez-Lopez J, et al. Long-term prognostic significance of response in multiple myeloma after stem cell transplantation. *Blood*. 2011;118(3):529–534.
7. Bensinger WI. Role of autologous and allogeneic stem cell transplantation in myeloma. *Leukemia*. 2009;23(3):442–448.
8. Lu X, et al. Alkylating agent melphalan augments the efficacy of adoptive immunotherapy using tumor-specific CD4+ T cells. *J Immunol*. 2015;194(4):2011–2021.
9. Chesi M, et al. Drug response in a genetically engineered mouse model of multiple myeloma is predictive of clinical efficacy. *Blood*. 2012;120(2):376–385.
10. Longsworth LG, Shedlovsky T, Macinnes DA. Electrophoretic patterns of normal and pathological human blood serum and plasma. *J Exp Med*. 1939;70(4):399–413.
11. Sathe P, et al. Innate immunodeficiency following genetic ablation of Mcl1 in natural killer cells. *Nat Commun*. 2014;5:4539.
12. Miller A, et al. High somatic mutation and neoantigen burden are correlated with decreased progression-free survival in multiple myeloma. *Blood Cancer J*. 2017;7(9):e612.
13. Lawrence MS, et al. Discovery and saturation analysis of cancer genes across 21 tumour types. *Nature*. 2014;505(7484):495–501.
14. Lohr JG, et al. Widespread genetic heterogeneity in multiple myeloma: implications for targeted therapy. *Cancer Cell*. 2014;25(1):91–101.
15. Inozume T, et al. Selection of CD8+PD-1+ lymphocytes in fresh human melanomas enriches for tumor-reactive T cells. *J Immunother*. 2010;33(9):956–964.
16. Fourcade J, et al. Upregulation of Tim-3 and PD-1 expression is associated with tumor antigen-specific CD8+ T cell dysfunction in melanoma patients. *J Exp Med*. 2010;207(10):2175–2186.
17. Pauken KE, Wherry EJ. Overcoming T cell exhaustion in infection and cancer. *Trends Immunol*. 2015;36(4):265–276.
18. Kaech SM, Wherry EJ. Heterogeneity and cell-fate decisions in effector and memory CD8$^+$ T cell differentiation during viral infection. *Immunity*. 2007;27(3):393–405.
19. Zhang X, Sun S, Hwang I, Tough DF, Sprent J. Potent and selective stimulation of memory-phenotype CD8+ T cells in vivo by IL-15. *Immunity*. 1998;8(5):591–599.
20. Guillerey C, et al. Immunosurveillance and therapy of multiple myeloma are CD226 dependent. *J Clin Invest*. 2015;125(5):2077–2089.
21. Miles JJ, Douek DC, Price DA. Bias in the αβ T-cell repertoire: implications for disease pathogenesis and vaccination. *Immunol Cell Biol*. 2011;89(3):375–387.
22. Prabhala RH, et al. Elevated IL-17 produced by TH17 cells promotes myeloma cell growth and inhibits immune function in multiple myeloma. *Blood*. 2010;115(26):5385–5392.
23. Prabhala RH, et al. Targeting IL-17A in multiple myeloma: a potential novel therapeutic approach in myeloma. *Leukemia*. 2016;30(2):379–389.
24. Veldhoen M, Hocking RJ, Atkins CJ, Locksley RM, Stockinger B. TGFbeta in the context of an inflammatory cytokine milieu supports de novo differentiation of IL-17-producing T cells. *Immunity*. 2006;24(2):179–189.
25. Hilbert DM, Kopf M, Mock BA, Köhler G, Rudikoff S. Interleukin 6 is essential for in vivo development of B lineage neoplasms. *J Exp Med*. 1995;182(1):243–248.
26. Varelias A, et al. Lung parenchyma-derived IL-6 promotes IL-17A-dependent acute lung injury after allogeneic stem cell transplantation. *Blood*. 2015;125(15):2435–2444.
27. Rawstron AC, et al. The interleukin-6 receptor alpha-chain (CD126) is expressed by neoplastic but not normal plasma cells. *Blood*. 2000;96(12):3880–3886.
28. Hirota K, et al. Fate mapping of IL-17-producing T cells in inflammatory responses. *Nat Immunol*. 2011;12(3):255–263.
29. Varelias A, et al. Acute graft-versus-host disease is regulated by an IL-17-sensitive microbiome. *Blood*. 2017;129(15):2172–2185.
30. Landrette SF, Madera D, He F, Castilla LH. The transcription factor PlagL2 activates Mpl transcription and signaling in hematopoietic progenitor and leukemia cells. *Leukemia*. 2011;25(4):655–662.
31. Landrette SF, et al. Plag1 and Plagl2 are oncogenes that induce acute myeloid leukemia in cooperation with Cbfb-MYH11. *Blood*. 2005;105(7):2900–2907.
32. Bradley E, et al. Critical role of Spns2, a sphingosine-1-phosphate transporter, in lung cancer cell survival and migration. *PLoS One*. 2014;9(10):e110119.
33. Hsu J, Sage J. Novel functions for the transcription factor E2F4 in development and disease. *Cell Cycle*. 2016;15(23):3183–3190.
34. Ichiba T, et al. Early changes in gene expression profiles of hepatic GVHD uncovered by oligonucleotide microarrays. *Blood*. 2003;102(2):763–771.
35. Yonezawa A, Dutt S, Chester C, Kim J, Kohrt HE. Boosting cancer immunotherapy with anti-CD137 antibody therapy. *Clin Cancer Res*. 2015;21(14):3113–3120.
36. Philip M, et al. Chromatin states define tumour-specific T cell dysfunction and reprogramming. *Nature*. 2017;545(7655):452–456.
37. Bruno B, et al. A comparison of allografting with autografting for newly diagnosed myeloma. *N Engl J Med*. 2007;356(11):1110–1120.
38. Kuehl WM, Bergsagel PL. Molecular pathogenesis of multiple myeloma and its premalignant precursor. *J Clin Invest*. 2012;122(10):3456–3463.
39. Mittal D, Gubin MM, Schreiber RD, Smyth MJ. New insights into cancer immunoediting and its three component phases--elimination, equilibrium and escape. *Curr Opin Immunol*. 2014;27:16–25.
40. Guillerey C, Nakamura K, Vuckovic S, Hill GR, Smyth MJ. Immune responses in multiple myeloma: role of the natural immune surveillance and potential of immunotherapies. *Cell Mol Life Sci*. 2016;73(8):1569–1589.
41. Pratt G, Goodyear O, Moss P. Immunodeficiency and immunotherapy in multiple myeloma. *Br J Haematol*. 2007;138(5):563–579.
42. Davies FE, et al. Thalidomide and immunomodulatory derivatives augment natural killer cell cytotoxicity in multiple myeloma. *Blood*. 2001;98(1):210–216.
43. Hayashi T, et al. Molecular mechanisms whereby immunomodulatory drugs activate natural killer cells: clinical application. *Br J Haematol*. 2005;128(2):192–203.
44. Carbone E, et al. HLA class I, NKG2D, and natural cytotoxicity receptors regulate multiple myeloma cell recognition by natural killer cells. *Blood*. 2005;105(1):251–258.
45. Pessoa de Magalhães RJ, et al. Analysis of the immune system of multiple myeloma patients achieving long-term disease control by multidimensional flow cytometry. *Haematologica*. 2013;98(1):79–86.
46. Suen H, et al. Multiple myeloma causes clonal T-cell immunosenescence: identification of potential novel targets for promoting tumour immunity and implications for checkpoint blockade. *Leukemia*. 2016;30(8):1716–1724.
47. Dhodapkar MV, Krasovsky J, Olson K. T cells from the tumor microenvironment of patients with progressive myeloma can generate strong, tumor-specific cytolytic responses to autologous, tumor-loaded dendritic cells. *Proc Natl Acad Sci U S A*. 2002;99(20):13009–13013.
48. Hayashi T, et al. Ex vivo induction of multiple myeloma-specific cytotoxic T lymphocytes. *Blood*. 2003;102(4):1435–1442.
49. Brown RD, et al. Prognostically significant cytotoxic T cell clones are stimulated after thalidomide therapy in patients with multiple myeloma. *Leuk Lymphoma*. 2009;50(11):1860–1864.
50. Minnie SA, et al. Myeloma escape after stem cell transplantation is a consequence of T-cell exhaustion and is prevented by TIGIT blockade. *Blood*. 2018;132(16):1675–1688.
51. Serody JS, Hill GR. The IL-17 differentiation pathway and its role in transplant outcome. *Biol Blood Marrow Transplant*. 2012;18(1 Suppl):S56–S61.
52. Kennedy GA, et al. Addition of interleukin-6 inhibition with tocilizumab to standard graft-versus-host disease prophylaxis after allogeneic stem-cell transplantation: a phase 1/2 trial. *Lancet Oncol*. 2014;15(13):1451–1459.
53. Li Y, et al. Potential relationship and clinical significance of miRNAs and Th17 cytokines in patients with multiple myeloma. *Leuk Res*. 2014;38(9):1130–1135.
54. Alexandrakis MG, et al. Serum interleukin-17 and its relationship to angiogenic factors in multiple myeloma. *Eur J Intern Med*. 2006;17(6):412–416.
55. Bryant C, et al. Long-term survival in multiple myeloma is associated with a distinct immunological profile, which includes proliferative cytotoxic T-cell clones and a favourable Treg/Th17 balance. *Blood Cancer J*. 2013;3:e148.
56. Palumbo A, Bruno B, Boccadoro M, Pileri A. Interferon-gamma in multiple myeloma. *Leuk Lymphoma*. 1995;18(3-4):215–219.
57. Frassanito MA, Cusmai A, Dammacco F. Deregulated cytokine network and defective Th1 immune response in multiple myeloma. *Clin Exp Immunol*. 2001;125(2):190–197.
58. Melero I, et al. Monoclonal antibodies against the 4-1BB T-cell activation molecule eradicate estab-

lished tumors. *Nat Med*. 1997;3(6):682–685.
59. Westwood JA, et al. Combination anti-CD137 and anti-CD40 antibody therapy in murine myc-driven hematological cancers. *Leuk Res*. 2014;38(8):948–954.
60. Murillo O, et al. Therapeutic antitumor efficacy of anti-CD137 agonistic monoclonal antibody in mouse models of myeloma. *Clin Cancer Res*. 2008;14(21):6895–6906.
61. Gahrton G, et al. Syngeneic transplantation in multiple myeloma - a case-matched comparison with autologous and allogeneic transplantation. European Group for Blood and Marrow Transplantation. *Bone Marrow Transplant*. 1999;24(7):741–745.
62. Bashey A, et al. Comparison of twin and autologous transplants for multiple myeloma. *Biol Blood Marrow Transplant*. 2008;14(10):1118–1124.
63. Galimberti S, et al. Peripheral blood stem cell contamination evaluated by a highly sensitive molecular method fails to predict outcome of autotransplanted multiple myeloma patients. *Br J Haematol*. 2003;120(3):405–412.
64. Gupta D, et al. CD34+-selected peripheral blood progenitor cell transplantation in patients with multiple myeloma: tumour cell contamination and outcome. *Br J Haematol*. 1999;104(1):166–177.
65. Stewart AK, et al. Purging of autologous peripheral-blood stem cells using CD34 selection does not improve overall or progression-free survival after high-dose chemotherapy for multiple myeloma: results of a multicenter randomized controlled trial. *J Clin Oncol*. 2001;19(17):3771–3779.
66. Alici E, et al. Long-term follow-up of gene-marked $CD34^+$ cells after autologous stem cell transplantation for multiple myeloma. *Cancer Gene Ther*. 2007;14(3):227–232.
67. Leonardi C, et al. Anti-interleukin-17 monoclonal antibody ixekizumab in chronic plaque psoriasis. *N Engl J Med*. 2012;366(13):1190–1199.
68. Genovese MC, et al. LY2439821, a humanized anti-interleukin-17 monoclonal antibody, in the treatment of patients with rheumatoid arthritis: A phase I randomized, double-blind, placebo-controlled, proof-of-concept study. *Arthritis Rheum*. 2010;62(4):929–939.
69. Hueber W, et al. Effects of AIN457, a fully human antibody to interleukin-17A, on psoriasis, rheumatoid arthritis, and uveitis. *Sci Transl Med*. 2010;2(52):52ra72.
70. Cooke RE, et al. Spontaneous onset and transplant models of the Vk*MYC mouse show immunological sequelae comparable to human multiple myeloma. *J Transl Med*. 2016;14:259.
71. Markey KA, et al. Soluble lymphotoxin is an important effector molecule in GVHD and GVL. *Blood*. 2010;115(1):122–132.
72. MacDonald KP, et al. Donor pretreatment with progenipoietin-1 is superior to granulocyte colony-stimulating factor in preventing graft-versus-host disease after allogeneic stem cell transplantation. *Blood*. 2003;101(5):2033–2042.
73. Chesi M, et al. AID-dependent activation of a MYC transgene induces multiple myeloma in a conditional mouse model of post-germinal center malignancies. *Cancer Cell*. 2008;13(2):167–180.
74. Cooke KR, et al. An experimental model of idiopathic pneumonia syndrome after bone marrow transplantation: I. The roles of minor H antigens and endotoxin. *Blood*. 1996;88(8):3230–3239.